

CERN-EP-2021-061
2021/09/03

CMS-HIG-20-009

Search for lepton-flavor violating decays of the Higgs boson in the $\mu\tau$ and $e\tau$ final states in proton-proton collisions at $\sqrt{s} = 13$ TeV

The CMS Collaboration*

Abstract

A search is presented for lepton-flavor violating decays of the Higgs boson to $\mu\tau$ and $e\tau$. The data set corresponds to an integrated luminosity of 137 fb^{-1} collected at the LHC in proton-proton collisions at a center-of-mass energy of 13 TeV. No significant excess has been found, and the results are interpreted in terms of upper limits on lepton-flavor violating branching fractions of the Higgs boson. The observed (expected) upper limits on the branching fractions are, respectively, $\mathcal{B}(\text{H} \rightarrow \mu\tau) < 0.15$ (0.15)% and $\mathcal{B}(\text{H} \rightarrow e\tau) < 0.22$ (0.16)% at 95% confidence level.

"Published in Physical Review D as doi:10.1103/PhysRevD.104.032013."

1 Introduction

One of the main goals of the LHC program is to search for processes beyond the standard model (BSM). The properties and decays of the Higgs boson (H) are thus far consistent with expectations of the standard model (SM) [1–6]. However, there is considerable motivation to search for BSM decays of the Higgs boson. The lepton-flavor violating (LFV) decays of the Higgs boson [7–9] can provide possible signatures of such processes. A previous investigation of the combined results from the CMS experiment constrained the branching fraction for $\mathcal{B}(H \rightarrow \text{BSM})$ to <0.36 at the 95% confidence level (CL), leaving the possibility for a large contribution for these decays [10].

The LFV decays $H \rightarrow e\mu$, $H \rightarrow e\tau$, or $H \rightarrow \mu\tau$ are forbidden in the SM, but take place through the LFV Yukawa couplings $Y_{e\mu}$, $Y_{e\tau}$, or $Y_{\mu\tau}$, respectively [11]. The LFV decays arise in models with more than one Higgs boson doublet [12], certain supersymmetric models [13–15], composite Higgs models [16, 17], models with flavor symmetries [18], the Randall–Sundrum model of extra spatial dimensions [19–23], and other models [24–29].

Here we report a search for LFV decays of the Higgs boson in the $\mu\tau$ and $e\tau$ channels performed using data collected by the CMS experiment in proton-proton (pp) collisions at a center-of-mass energy of 13 TeV during the 2016–2018 data-taking period, corresponding to an integrated luminosity of 137 fb^{-1} . The CMS experiment set upper limits of 0.25% and 0.61% [30] and the ATLAS experiment set upper limits of 0.28% and 0.47% [31] on $\mathcal{B}(H \rightarrow \mu\tau)$ and $\mathcal{B}(H \rightarrow e\tau)$ at 95% CL, respectively, based on the 2016 data set, corresponding to an integrated luminosity of 36 fb^{-1} .

The presence of an LFV Higgs boson coupling leads to processes such as $\mu \rightarrow e$, $\tau \rightarrow \mu$, and $\tau \rightarrow e$ to proceed via a virtual Higgs boson [32, 33]. The experimental limits on these decays yield indirect constraints on $\mathcal{B}(H \rightarrow e\mu)$, $\mathcal{B}(H \rightarrow \mu\tau)$, and $\mathcal{B}(H \rightarrow e\tau)$ [11, 34]. The null result for $\mu \rightarrow e\gamma$ [35] strongly constrains $\mathcal{B}(H \rightarrow e\mu)$ to $< 10^{-8}$. Searches for rare τ lepton decays [36], such as $\tau \rightarrow e\gamma$ and $\tau \rightarrow \mu\gamma$, and the measurement of the electron and muon magnetic moments, have set constraints on $\mathcal{B}(H \rightarrow e\tau)$ and $\mathcal{B}(H \rightarrow \mu\tau)$ of $\approx 10\%$, which are much less stringent than those from the direct searches.

Our search is performed in the $\mu\tau_{h'}$, $\mu\tau_{e'}$, $e\tau_{h'}$, and $e\tau_{\mu}$ channels, where $\tau_{h'}$, $\tau_{e'}$, and τ_{μ} correspond to the $\tau \rightarrow$ hadrons, electron, and muon decay channels of τ leptons, respectively, each accompanied by its corresponding neutrinos. The $e\tau_e$ and $\mu\tau_{\mu}$ decays are not considered because of the large background contribution from Z/γ^* decays.

Our search significantly improves the sensitivity relative to similar previous studies [30, 31, 37]. The search makes use of boosted decision tree (BDT) discriminants to distinguish signal from background in the distributions which are then used for performing the statistical analysis. Constraints on the branching fractions are extracted under the assumption that only one of the LFV decays contributes additionally to the SM Higgs boson total width. The constraints on the branching fractions are correspondingly translated into limits on the $Y_{e\tau}$ and $Y_{\mu\tau}$ LFV Yukawa couplings.

This paper is organized as follows: a description of the CMS detector is given in Section 2, collision data and simulated events are discussed in Section 3, event reconstruction is described in Section 4, and event selection is described separately for the four decay channels in Section 5. Background estimation and systematic uncertainties are described in Sections 6 and 7, respectively. Results are presented in Section 8 and the paper is summarized in Section 9.

2 The CMS detector

The CMS detector consists of a silicon pixel and strip tracker, a lead tungstate crystal electromagnetic calorimeter (ECAL), a brass and scintillator hadron calorimeter (HCAL), and a muon system composed of gaseous detectors. Each subdetector consists of a barrel and two endcap sections. The central feature of the CMS detector is a superconducting solenoid of 6 m internal diameter, providing a magnetic field of 3.8 T. The tracking systems and the calorimeters are contained within the solenoid volume; the muon chambers are embedded in the steel flux-return yoke outside the solenoid. Forward calorimeters extend the pseudorapidity (η) coverage provided by the barrel and endcap detectors.

Events of interest are selected using a two-tiered trigger system. The first level, composed of custom hardware processors, uses information from the calorimeters and muon detectors to select events at a rate of ≈ 100 kHz within a fixed latency of $\approx 4 \mu\text{s}$ [38]. The second level, the high-level trigger, consists of a farm of processors running a version of the full event reconstruction software optimized for fast processing that reduces the event rate to ≈ 1 kHz before data storage [39]. A more detailed description of the CMS detector, together with a definition of the coordinate system and kinematic variables, can be found in Ref. [40].

3 Collision data and simulated events

The search presented makes use of pp collisions collected at the CMS experiment at a center-of-mass energy of 13 TeV in 2016–2018. The total integrated luminosity amounted to 35.9 fb^{-1} in 2016, 41.5 fb^{-1} in 2017, and 59.7 fb^{-1} in 2018. Single-muon triggers with isolation criteria are used to collect the data in the $\mu\tau_h$ channel. Electron-muon triggers are used to collect data in the $\mu\tau_e$ and $e\tau_\mu$ channels. Triggers requiring a single isolated electron, or a combination of an electron and τ_h , are used in the $e\tau_h$ channel. The trigger thresholds are mentioned in Section 5.

Simulated events are used to model signal and background events using several event generators. In all cases parton showering, hadronization, and underlying event properties are modeled using PYTHIA [41] version 8.212. The PYTHIA parameters affecting the description of the underlying event are set to the CUETP8M1 tune in 2016 [42], except for the $t\bar{t}$ events that use the CP5 tune which is used for all the events in 2017 and 2018 [43]. The NNPDF3.0 parton distribution functions (PDFs) for all 2016 events and the NNPDF3.1 PDFs for the 2017 and 2018 events [44].

The simulation of interactions in the CMS detector is based on GEANT4 [45], using the same reconstruction algorithms as used for data. The Higgs bosons are generated in pp collisions predominantly through gluon fusion (ggH) [46], but also via vector boson fusion (VBF) [47], and in association with a vector boson (W or Z) [48]. Such events are generated at next-to-leading order (NLO) in perturbative quantum chromodynamics (QCD) with the POWHEG v2.0 generator [49–54], using the implementation of Refs. [55, 56]. For the LFV signal, we consider just the Higgs bosons via the ggH and VBF mechanisms as the contribution from associated vector boson production is found to be negligible.

The $Z \rightarrow \tau\tau$ background events are estimated in a data-driven manner using the embedding technique because it provides a better description of jets, pileup, as well as detector noise and resolution effects compared to simulation. These events are obtained from data with well identified $Z \rightarrow \mu\mu$ decays from which muons are removed, and simulated τ leptons are embedded with the same kinematic variables as the replaced muons. The MADGRAPH5_aMC@NLO generator [57] (version 2.2.2 in 2016, version 2.4.2 in 2017 and 2018) is used to simulate the

$Z \rightarrow ee+\text{jets}$ and $Z \rightarrow \mu\mu+\text{jets}$ processes, the $W+\text{jets}$ background process, and the electroweak (EW) W/Z events. They are simulated at leading order with the MLM jet matching and merging schemes [58].

Diboson production is simulated at NLO using the MADGRAPH5_aMC@NLO generator with the FxFx jet-matching and merging scheme [59]. Top quark-antiquark pair and single top quark production are generated at NLO using POWHEG.

The effect of pileup, where events of interest have multiple pp interactions in the same bunch crossing, is taken into account in simulated events by generating concurrent minimum bias events. All simulated events are weighted to match the pileup distribution observed in the data.

4 Event reconstruction

The particle flow (PF) algorithm [60] reconstructs and identifies each particle in an event through an optimized combination of information from the various subdetectors of the CMS detector. In this process, identifying the PF candidate type (photons, electrons, muons, charged, and neutral hadrons) plays an important role in determining particle direction and energy. The candidate vertex with the largest value of summed physics object p_T^2 , where p_T is the transverse momentum, is taken to be the primary pp interaction vertex (PV). The physics objects are returned by a jet finding algorithm [61, 62] applied to all charged tracks associated with the vertex, plus the corresponding associated missing transverse momentum (\vec{p}_T^{miss}).

An electron is identified as a track from the PV combined with one or more ECAL energy clusters. These clusters correspond to the electron and possible bremsstrahlung photons emitted when passing through the tracker. Electrons are accepted in the range $|\eta| < 2.5$, except for the region $1.44 < |\eta| < 1.57$ where the detector's service infrastructure is located. They are identified with an efficiency of 80% using a multivariate discriminator that combines observables sensitive to the amount of bremsstrahlung energy deposited along the electron trajectory, the geometric and momentum matching between the electron trajectory and associated clusters, and the distribution in shower energy in the calorimeters [63]. Electrons from photon conversions are removed. The electron momentum is estimated by combining the energy measurement in the ECAL with the momentum measurement in the tracker. The momentum resolution for electrons with $p_T \approx 45$ GeV from $Z \rightarrow ee$ decays ranges from 1.7 to 4.5% depending on the $|\eta|$. It is generally better in the barrel region than in the endcaps [64].

Muons are measured in the $|\eta| < 2.4$ range using the drift tube, cathode strip chamber, and resistive plate chamber technologies. The efficiency to reconstruct and identify muons is greater than 96%. Matching muons to tracks measured in the silicon tracker results in a relative p_T resolution for muons with p_T up to 100 GeV of 1% in the barrel and 3% in the endcaps [65].

The muon or electron isolations are measured relative to its p_T^ℓ , where ℓ is either μ or e , values by summing over the scalar p_T of PF particles in a cone of $\Delta R = 0.4$ or 0.3 around the lepton:

$$I_{\text{rel}}^\ell = \left(\sum p_T^{\text{PV charged}} + \max \left[0, \sum p_T^{\text{neutral}} + \sum p_T^\gamma - p_T^{\text{PU}}(\ell) \right] \right) / p_T^\ell,$$

where $p_T^{\text{PV charged}}$, p_T^{neutral} , and p_T^γ indicate the p_T of a charged hadron, a neutral hadron, and a photon within the cone, respectively. The neutral particle contribution to isolation from pileup, $p_T^{\text{PU}}(\ell)$, is estimated from the area of jet and its median energy density in the event [66] for the electron. For the muon, half of the p_T sum of charged hadrons within the isolation cone, not

originating from the PV, is used instead. The charged-particle contribution to isolation from the pileup is rejected by requiring the tracks to originate from the PV.

The reconstruction of τ_h is performed using the hadrons-plus-strips algorithm, which combines the signature for charged hadrons composed of tracks left in the tracker and energy depositions in the calorimeters with the signature for electrons or photons from neutral pion decays that are reconstructed as electromagnetic “strips” in η - ϕ space [67], where ϕ is the azimuth in radians. The combination of these signatures provides the four-vector for the parent τ_h . Based on the overall neutral versus charged contents of the τ_h reconstruction, a decay mode is assigned as h^\pm , $h^\pm\pi^0$, $h^\pm h^\mp h^\pm$, or $h^\pm h^\mp h^\pm\pi^0$, where h^\pm denotes a charged hadron. It has a reconstruction efficiency of $\approx 80\%$.

The τ_h reconstructed using the hadrons-plus-strips algorithm must be well identified to reject jets, muons, and electrons misidentified as τ_h . A deep neural network (DNN) discriminator is used to further improve τ_h identification [68]. The input variables to the DNN include τ_h lifetime, isolation, and information of PF candidates reconstructed within the τ lepton signal or isolation cones. A p_T dependent threshold on the output of the DNN is used to distinguish τ_h from jets. The chosen working point (WP) has a τ_h identification efficiency of 70% with a misidentification probability of 1%. The DNN can reject electrons and muons misidentified as τ_h using dedicated criteria based on the consistency between the tracker, calorimeter, and muon detector measurements. In the $\mu\tau_h$ or $e\tau_h$ channel, we use a WP that has an efficiency of 97.5% or 87.5% with a misidentification probability of 1–2% or 0.2–0.3% to discriminate τ_h against electrons, and we use a WP that has an efficiency of 99.6% or 99.8% with a misidentification probability of 0.04% or 0.06% to discriminate τ_h against muons, respectively.

Charged hadrons are defined as PF tracks from the PV not reconstructed as electrons, muons, or τ_h leptons. Neutral hadrons are identified as HCAL energy clusters not assigned to any charged hadron or as excesses in ECAL or HCAL energies relative to the small charged-hadron energy deposit. All the PF hadron candidates are clustered into jets using the infrared- and collinear-safe anti- k_T algorithm [61] with a distance parameter of 0.4. Jet momentum is determined as the vectorial sum of all particle momenta in the jet. It is found from simulation to be, on average, within 5–10% of the true momentum over the entire p_T spectrum and detector acceptance [69]. Jets that contain b quarks are tagged using a DNN-based algorithm, using a WP with efficiency of 70% for a misidentification probability for light-flavor jets of 1% [70].

The interactions from pileup add more tracks and calorimetric energy depositions, thereby increasing the apparent jet momenta. To mitigate this effect, tracks identified as originating from pileup vertices are discarded, and an offset correction is applied to correct the remaining contributions [71]. Jet energy corrections are obtained from simulation studies so that the average measured energy of jets matches that of particle level jets. In-situ measurements of the momentum balance in photon+jet, Z+jets, and multijet events are used to determine any residual differences between the jet energy scale in data and simulation, and appropriate corrections are applied [72]. Additional selection criteria are applied to each jet to remove jets potentially dominated by instrumental effects or reconstruction failures. When combining information from the entire detector, the jet energy resolution typically amounts to 15% at 10 GeV, 8% at 100 GeV, and 4% at 1 TeV. The variable $\Delta R = \sqrt{(\Delta\eta)^2 + (\Delta\phi)^2}$ is used to measure the separation between reconstructed objects in the detector. Any jet within $\Delta R = 0.5$ of identified leptons is removed. The reconstructed jets must have a $p_T > 30$ GeV and $|\eta| < 4.7$. Data collected in the high $|\eta|$ region of the ECAL endcaps were affected by noise during the 2017 data taking. This is mitigated by discarding events containing jets with $p_T < 50$ GeV and $2.65 < |\eta| < 3.14$ in the 2017 data.

The vector \vec{p}_T^{miss} is computed as the negative of the vector p_T sum of all the PF candidates in an event, and its magnitude is denoted as p_T^{miss} [73]. The \vec{p}_T^{miss} is modified to account for corrections to the reconstructed jets' energy scale in the event. Anomalous high- p_T^{miss} events can originate from various reconstruction failures, detector malfunctions, or backgrounds not from beam-beam sources. Such events are rejected using event filters designed to identify more than 85–90% of the spurious high- p_T^{miss} events with a mistag rate of less than 0.1% [73]. In addition to the event-filtering algorithms, we require the jets to have a neutral hadron energy fraction smaller than 0.9, which rejects more than 99% of jets due to detector noise, independent of jet p_T , with a negligible mistag rate. Corrections applied to the \vec{p}_T^{miss} reduce the mismodeling of \vec{p}_T^{miss} in simulated Z, W, and Higgs boson events. The corrections are applied to simulated events based on the vectorial difference in the measured \vec{p}_T^{miss} and total p_T of neutrinos originating from the decay of the Z, W, or Higgs bosons. Their average effect is the reduction of the magnitude of the \vec{p}_T^{miss} obtained from the simulation by a few GeV.

5 Event selection

The signal topology consists of a muon or an electron and an oppositely charged τ lepton. The events in the $\mu\tau$ and $e\tau$ channels are further divided into leptonic and hadronic channels based on the τ lepton decay mode (τ_μ , τ_e , or τ_h). Jets misidentified as electrons or muons are suppressed by imposing isolation requirements described above. A set of loose selection criteria, known as the 'preselection', is first defined in each channel's respective signature. Events with more than two jets are not considered in the search. Each channel's events are then divided into categories based on the number of jets in the event (0-, 1-, or 2-jet) to enhance different Higgs boson production mechanisms. The dominant production mechanism contributing to the signal yield in the 0-jet category is ggH, while in the 1-jet category, it is ggH with initial-state radiation. The 2-jet category is further split into two based on the invariant mass of the two jets (m_{jj}). The optimization resulted in a threshold of 550 GeV and 500 GeV on m_{jj} for the $\mu\tau$ and $e\tau$ channels, respectively, for the sensitivity optimization. The dominant production mechanism is ggH with initial-state radiation for events with $m_{jj} < 550$ GeV and < 500 GeV, while it is VBF for events with $m_{jj} > 550$ GeV and > 500 GeV for the $\mu\tau$ and $e\tau$ channels, respectively.

A variable providing an estimate of m_H using the observed decay products of the Higgs boson, the collinear mass, is defined as $m_{\text{col}} = m_{\text{vis}} / \sqrt{x_\tau^{\text{vis}}}$, where m_{vis} is the visible invariant mass of the τ - μ or τ - e system and x_τ^{vis} is the fraction of the τ lepton p_T carried by the visible decay products of the τ lepton ($\vec{\tau}^{\text{vis}}$). The definition is based on the "collinear approximation" with the observation that, since $m_H \gg m_\tau$, the τ lepton decay products are Lorentz-boosted in the direction of the τ lepton [74]. The momentum of neutrino(s) from the τ lepton decay can be approximated to have the same direction as the $\vec{\tau}^{\text{vis}}$. The component of the \vec{p}_T^{miss} in the direction of the $\vec{\tau}^{\text{vis}}$ is used to estimate the transverse component of the neutrino momentum ($p_T^{\vec{v},\text{est}}$). This information is combined to estimate the x_τ^{vis} which is defined as $x_\tau^{\text{vis}} = p_T^{\vec{\tau}^{\text{vis}}} / (p_T^{\vec{\tau}^{\text{vis}}} + p_T^{\vec{v},\text{est}})$. The collinear mass distributions of simulated signal, data, and backgrounds in each channel are shown in Fig. 1.

The transverse mass $m_T(\ell)$ is a variable constructed from the lepton p_T and the \vec{p}_T^{miss} vectors: $m_T(\ell) = \sqrt{2|\vec{p}_T^\ell||\vec{p}_T^{\text{miss}}|(1 - \cos\Delta\phi_{\ell,\vec{p}_T^{\text{miss}}})}$, where $\Delta\phi_{\ell,\vec{p}_T^{\text{miss}}}$ is the angle in the transverse plane between the lepton and the \vec{p}_T^{miss} , used to discriminate the Higgs boson signal from the W+jets background. The $m_T(\ell)$ distribution for the signal defined using visible decay products of the τ lepton peaks at lower values, while it peaks at higher values for the W+jets background.

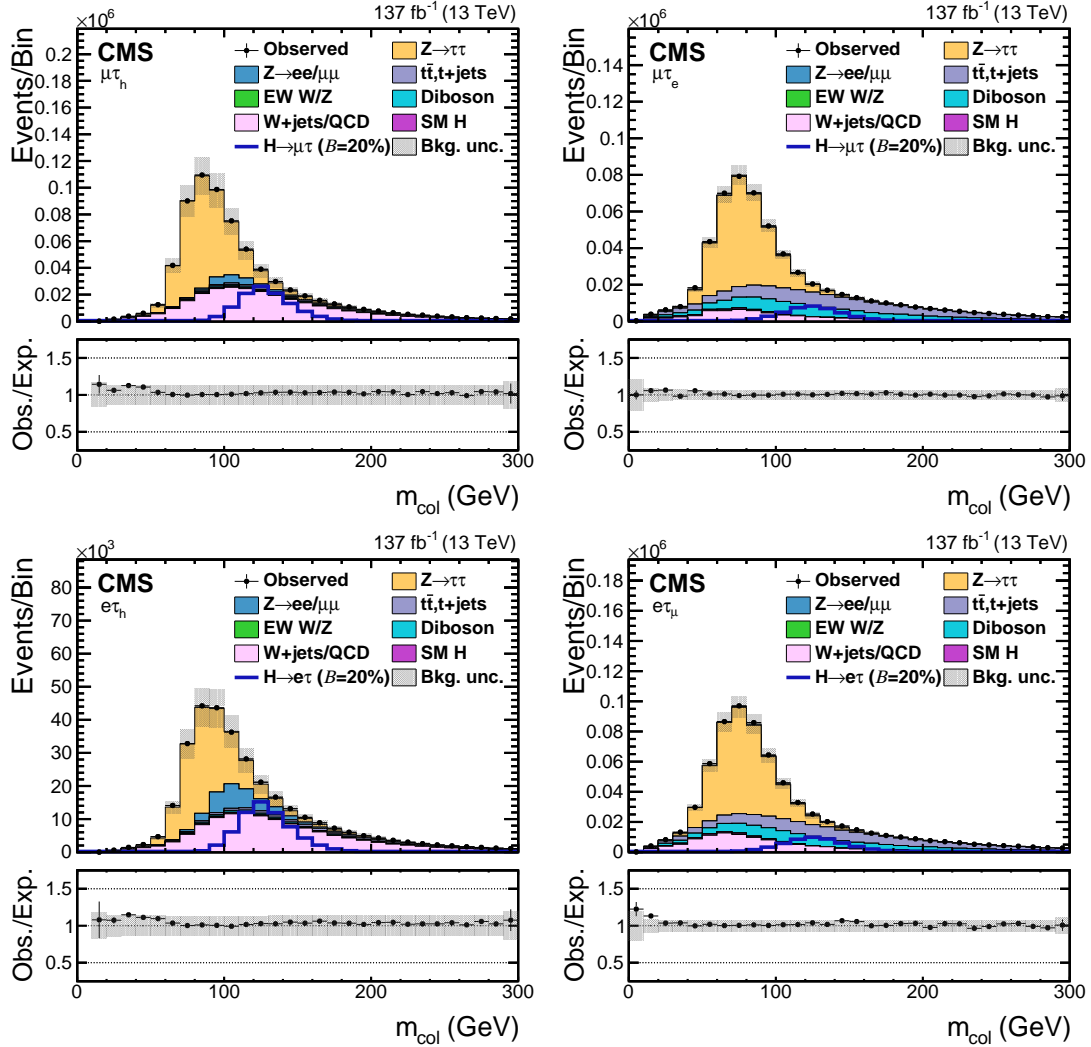


Figure 1: Collinear mass distributions for the data and background processes. A $\mathcal{B}(H \rightarrow \mu\tau) = 20\%$ and $\mathcal{B}(H \rightarrow e\tau) = 20\%$ are assumed for the two signal processes. The channels are $H \rightarrow \mu\tau_h$ (upper row left), $H \rightarrow \mu\tau_e$ (upper row right), $H \rightarrow e\tau_h$ (lower row left), and $H \rightarrow e\tau_\mu$ (lower row right). The lower panel in each plot shows the ratio of data and estimated background. The uncertainty band corresponds to the background uncertainty in which the statistical and systematic uncertainties are added in quadrature.

To improve discrimination between signal and background events, a BDT is trained using the TMVA toolkit of the ROOT analysis package [75]. A BDT is trained in each channel using a mixture of simulated signal events comprising the ggH and VBF processes, weighted according to their expected yield from SM production cross sections. In hadronic channels, the dominant sources of background come from the $Z \rightarrow \tau\tau$ process and events with misidentified leptons. The background used for training a BDT in the hadronic channels is obtained from data containing misidentified lepton events of the same electric charge for both the leptons and $Z \rightarrow \ell\ell$ ($\ell = e, \mu, \tau$) simulated events with their applied signal selections. In leptonic channels, the dominant sources of background come from the $Z \rightarrow \tau\tau$ process, the $t\bar{t}$ process, and events with misidentified leptons. The background used for training a BDT in the leptonic channels is obtained from $t\bar{t}$ and $Z \rightarrow \ell\ell$ simulated events mixed and weighted according to their expected yield from SM production cross sections. Additional background for training comes from events with misidentified leptons in a control region (CR) in data, where the isolation requirements are inverted with the same electric charge for both the leptons. A detailed description of the different background processes and their estimation is given in Section 6.

The input variables to the BDT are mentioned separately for each channel below. The input variables are chosen based on their separation power as observed during training the BDT. The trained BDT is validated in a dedicated background enriched validation region (VR) for each channel and is detailed in Section 6. In all the channels, events containing additional electrons, muons, or τ_h candidates are vetoed. Also, events with at least one b-tagged jet are rejected to suppress the $t\bar{t}$ background. After applying the selections, a maximum likelihood fit is performed to the BDT discriminant distributions in each channel. The various systematic uncertainties are incorporated as nuisance parameters in the fit. The BDT discriminant distributions in all the channels are shown after determining the best fit values of the nuisance parameters from the fit to the signal-plus-background hypothesis, as discussed later in Section 7.

5.1 $H \rightarrow \mu\tau_h$

In this channel, the preselection requires a muon and τ_h of opposite electric charge with a separation of $\Delta R > 0.5$. The trigger requires the presence of an isolated muon with a p_T threshold of 24 GeV. In 2017, this trigger is “prescaled”, which means that only a fraction of events selected will pass the trigger. Hence, it is used in conjunction with another trigger based on the presence of an isolated muon with a p_T threshold of 27 GeV. The muon is required to have $p_T > 26$ GeV, $|\eta| < 2.1$, and $I_{\text{rel}}^\mu < 0.15$. The τ_h is required to have $p_T > 30$ GeV and $|\eta| < 2.3$. The selections for the $\mu\tau_h$ channel are summarized in Table 1.

The input variables to the BDT are p_T^μ , $p_T^{\tau_h}$, m_{col} , \vec{p}_T^{miss} , $m_T(\tau, \vec{p}_T^{\text{miss}})$, $\Delta\eta(\mu, \tau_h)$, $\Delta\phi(\mu, \tau_h)$, and $\Delta\phi(\tau_h, \vec{p}_T^{\text{miss}})$. The neutrino is assumed to be collinear with τ_h , which motivates using the $\Delta\phi(\tau_h, \vec{p}_T^{\text{miss}})$ variable. The two leptons are usually produced in opposite directions of the azimuthal plane, which motivates using the $\Delta\phi(\mu, \tau_h)$ variable. The post-fit distributions of simulated signal, data, and backgrounds in each category of the $\mu\tau_h$ channel are shown in Fig. 2.

5.2 $H \rightarrow \mu\tau_e$

In this channel, the preselection requires a muon and electron of opposite electric charge with a separation of $\Delta R > 0.3$. The triggers require both a muon and an electron, where the muon has p_T above 23 GeV, and the electron has p_T above 12 GeV. The muon is required to have $p_T > 24$ GeV, $|\eta| < 2.4$, and $I_{\text{rel}}^\mu < 0.15$. The electron is required to have $p_T > 13$ GeV, $|\eta| < 2.5$, and $I_{\text{rel}}^e < 0.1$. The selections for the $\mu\tau_e$ channel are summarized in Table 1.

The input variables to the BDT are p_T^μ , p_T^e , m_{col} , $m_T(\mu, \vec{p}_T^{\text{miss}})$, $m_T(e, \vec{p}_T^{\text{miss}})$, $\Delta\phi(e, \mu)$, $\Delta\phi(\mu, \vec{p}_T^{\text{miss}})$, and $\Delta\phi(e, \vec{p}_T^{\text{miss}})$. The neutrinos are assumed to be collinear with the electron, which motivates using the $\Delta\phi(e, \vec{p}_T^{\text{miss}})$ variable. The two leptons are usually produced in opposite directions of the azimuthal plane, which motivates using the $\Delta\phi(e, \mu)$ variable. The post-fit distributions of simulated signal, data, and backgrounds in each category of the $\mu\tau_e$ channel are shown in Fig. 3.

Table 1: Event selection criteria for the $H \rightarrow \mu\tau$ channels.

| Variable | $\mu\tau_h$ | $\mu\tau_e$ |
|----------------------|-----------------------------------------------------------------------------|--------------------------------------------------------|
| p_T^e | — | $>13 \text{ GeV}$ |
| p_T^μ | $>26 \text{ GeV}$ | $>24 \text{ GeV}$ |
| $p_T^{\tau_h}$ | $>30 \text{ GeV}$ | — |
| $ \eta ^e$ | — | <2.5 |
| $ \eta ^\mu$ | <2.1 | <2.4 |
| $ \eta ^{\tau_h}$ | <2.3 | — |
| I_{rel}^e | — | <0.1 |
| I_{rel}^μ | <0.15 | <0.15 |
| Trigger requirement | $p_T^\mu > 24 \text{ GeV}$ (all years) $p_T^\mu > 27 \text{ GeV}$ (2017) | $p_T^e > 12 \text{ GeV}$ $p_T^\mu > 23 \text{ GeV}$ |

5.3 $H \rightarrow e\tau_h$

In this channel, the preselection requires an electron and τ_h of opposite electric charge with a separation of $\Delta R > 0.5$. The triggers require the presence of an isolated electron with a p_T threshold of 25 GeV (2016), 27 GeV (2017), or 32 GeV (2018). In 2017 and 2018, the signal acceptance is increased by selecting events where the electron has p_T above 24 GeV and the τ_h has p_T above 30 GeV. The electron is required to have $p_T > 27 \text{ GeV}$, $|\eta| < 2.1$, and $I_{\text{rel}}^e < 0.15$. The τ_h is required to have $p_T > 30 \text{ GeV}$ and $|\eta| < 2.3$. The selections for the $e\tau_h$ channel are summarized in Table 2.

The input variables to the BDT are p_T^e , $p_T^{\tau_h}$, m_{col} , m_{vis} , $m_T(\tau, \vec{p}_T^{\text{miss}})$, $\Delta\eta(e, \tau_h)$, $\Delta\phi(e, \tau_h)$, and $\Delta\phi(\tau_h, \vec{p}_T^{\text{miss}})$. As can be seen, the input variables are similar to $\mu\tau_h$ channel except for the addition of the variable m_{vis} and removing \vec{p}_T^{miss} . The variable m_{vis} has better separation power as the $e\tau_h$ channel has more $Z \rightarrow ee + \text{jets}$ background than the $Z \rightarrow \mu\mu + \text{jets}$ background in the $\mu\tau_h$ channel. The post-fit distributions of simulated signal, data, and backgrounds in each category of the $e\tau_h$ channel are shown in Fig. 4.

5.4 $H \rightarrow e\tau_\mu$

In this channel, the preselection requires an electron and muon of opposite electric charge with a separation of $\Delta R > 0.4$. The triggers require both an electron and a muon, where the electron has p_T above 23 GeV, and the muon has p_T above 8 GeV. The electron is required to have $p_T > 24 \text{ GeV}$, $|\eta| < 2.5$, and $I_{\text{rel}}^e < 0.1$. The muon is required to have $p_T > 10 \text{ GeV}$, $|\eta| < 2.4$, and $I_{\text{rel}}^\mu < 0.15$. The selections for the $e\tau_\mu$ channel are summarized in Table 2.

The input variables to the BDT are p_T^μ , p_T^e , m_{col} , m_{vis} , $m_T(\mu, \vec{p}_T^{\text{miss}})$, $\Delta\phi(e, \mu)$, $\Delta\phi(\mu, \vec{p}_T^{\text{miss}})$, and $\Delta\phi(e, \vec{p}_T^{\text{miss}})$. As can be seen, the input variables are similar to $\mu\tau_e$ channel except for the

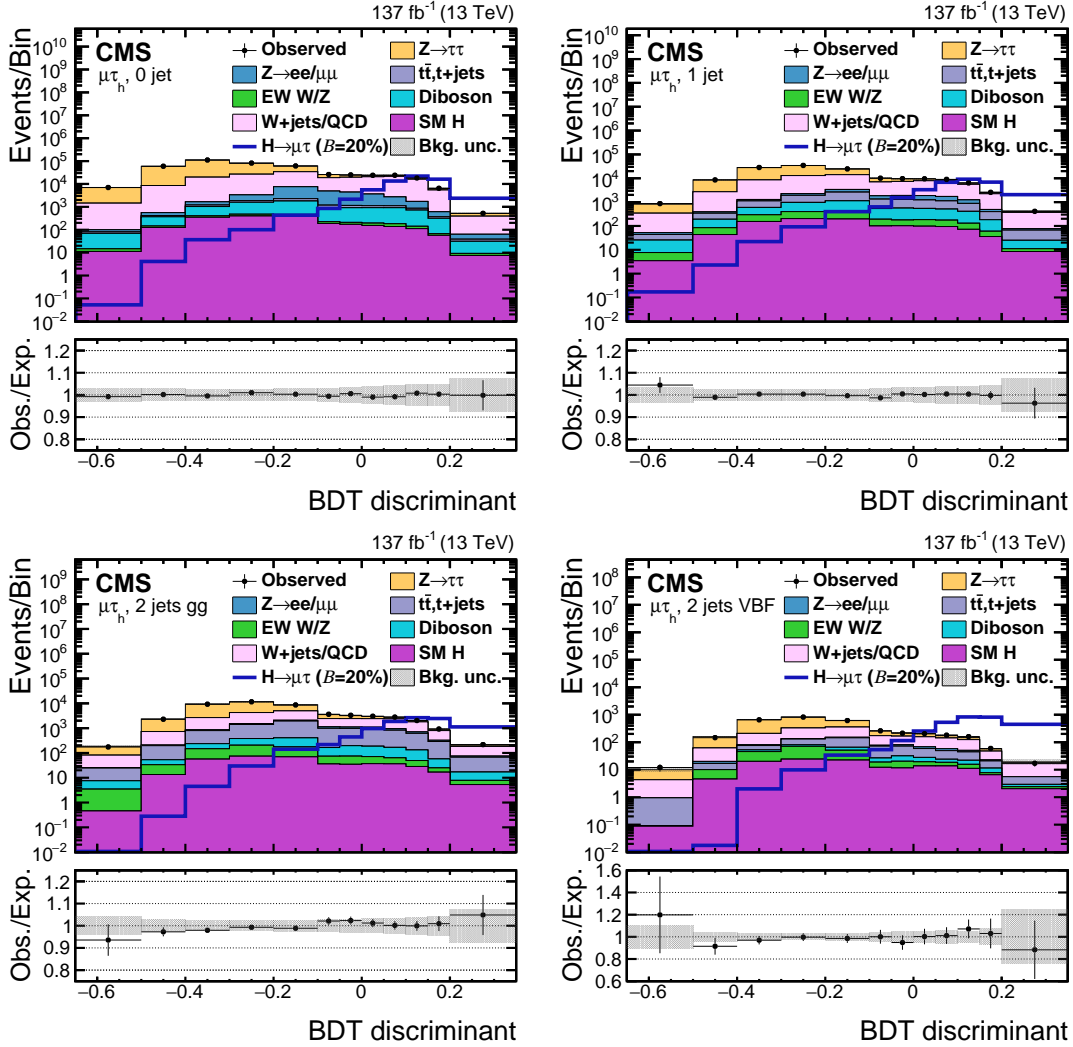


Figure 2: BDT discriminant distributions for the data and background processes in the $H \rightarrow \mu\tau_h$ channel. A $\mathcal{B}(H \rightarrow \mu\tau) = 20\%$ is assumed for the signal. The channel categories are 0 jets (upper row left), 1 jet (upper row right), 2 jets ggH (lower row left), and 2 jets VBF (lower row right). The lower panel in each plot shows the ratio of data and estimated background. The uncertainty band corresponds to the background uncertainty in which the post-fit statistical and systematic uncertainties are added in quadrature.

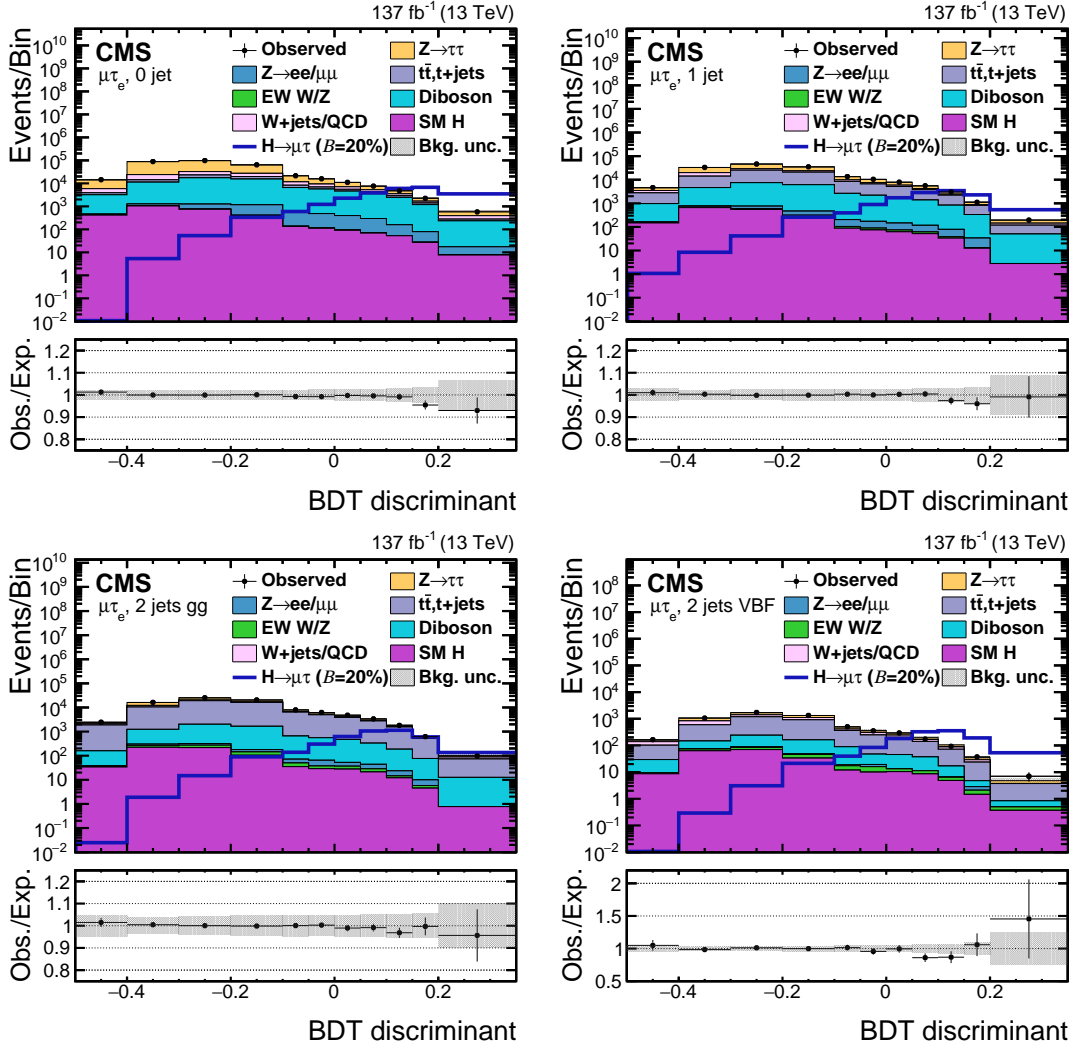


Figure 3: BDT discriminant distributions for the data and background processes in the $H \rightarrow \mu\tau_e$ channel. A $\mathcal{B}(H \rightarrow \mu\tau) = 20\%$ is assumed for the signal. The channel categories are 0 jets (upper row left), 1 jet (upper row right), 2 jets ggH (lower row left), and 2 jets VBF (lower row right). The lower panel in each plot shows the ratio of data and estimated background. The uncertainty band corresponds to the background uncertainty in which the post-fit statistical and systematic uncertainties are added in quadrature.

addition of the variable m_{vis} and removing $m_{\text{T}}(e, \vec{p}_{\text{T}}^{\text{miss}})$. The post-fit distributions of simulated signal, data, and backgrounds in each category of the $e\tau_{\mu}$ channel are shown in Fig. 5.

Table 2: Event selection criteria for the $H \rightarrow e\tau$ channels.

| Variable | $e\tau_{\text{h}}$ | $e\tau_{\mu}$ |
|----------------------------------|---------------------------------------------------------------------------------------------------------------|--------------------------------------------|
| p_{T}^{e} | $>27 \text{ GeV}$ | $>24 \text{ GeV}$ |
| p_{T}^{μ} | — | $>10 \text{ GeV}$ |
| $p_{\text{T}}^{\tau_{\text{h}}}$ | $>30 \text{ GeV}$ | — |
| $ \eta ^{\text{e}}$ | <2.1 | <2.5 |
| $ \eta ^{\mu}$ | — | <2.4 |
| $ \eta ^{\tau_{\text{h}}}$ | <2.3 | — |
| $I_{\text{rel}}^{\text{e}}$ | <0.15 | <0.1 |
| I_{rel}^{μ} | — | <0.15 |
| Trigger requirement | $p_{\text{T}}^{\text{e}} > 25 \text{ GeV}$ (2016) | |
| | $p_{\text{T}}^{\text{e}} > 27 \text{ GeV}$ (2017) | $p_{\text{T}}^{\text{e}} > 23 \text{ GeV}$ |
| | $p_{\text{T}}^{\text{e}} > 32 \text{ GeV}$ (2018) | $p_{\text{T}}^{\mu} > 8 \text{ GeV}$ |
| | $p_{\text{T}}^{\text{e}} > 24 \text{ GeV}$ and $p_{\text{T}}^{\tau_{\text{h}}} > 30 \text{ GeV}$ (2017, 2018) | |

6 Background estimation

One of the major background contributions comes from the $Z \rightarrow \tau\tau$ process, in which the muon or electron arises from a τ lepton decay. The other major background contributions arise from the W +jets process and from multijets events produced through the strong interaction (referred to as QCD multijet events hereafter), where one or more of the jets are misidentified as leptons. These backgrounds are estimated from data either fully or with the aid of simulation. The $t\bar{t}$ and single top quark background contributes substantially in leptonic channels and is estimated using simulated events along with the other backgrounds. The background estimates are validated in different orthogonal VRs constructed to have enhanced contributions from specific backgrounds.

6.1 $Z \rightarrow \tau\tau$ background

The $Z \rightarrow \tau\tau$ background is estimated from data using an embedding technique [76]. This technique allows for an estimation of the genuine $\tau\tau$ SM backgrounds from data with reduced simulation input. This minimizes the uncertainties that arise from using simulation. Events with a pair of oppositely charged muons are selected in data so that $Z \rightarrow \mu\mu$ events largely dominate. These data events are selected independently of the event selection criteria described in Section 5. The muons are removed from the selected events and replaced with simulated τ leptons with the same kinematic properties as those of the replaced muon. In that way, a set of hybrid events is obtained that relies on simulation only for the decay of the τ leptons. The description of the underlying event or the production of associated jets is taken entirely from data. This technique results in a more accurate description of the $\vec{p}_{\text{T}}^{\text{miss}}$ and jet-related variables than simulation and an overall reduction in the systematic uncertainties. Embedded events cover all backgrounds with two genuine τ leptons, and this includes a small fraction of

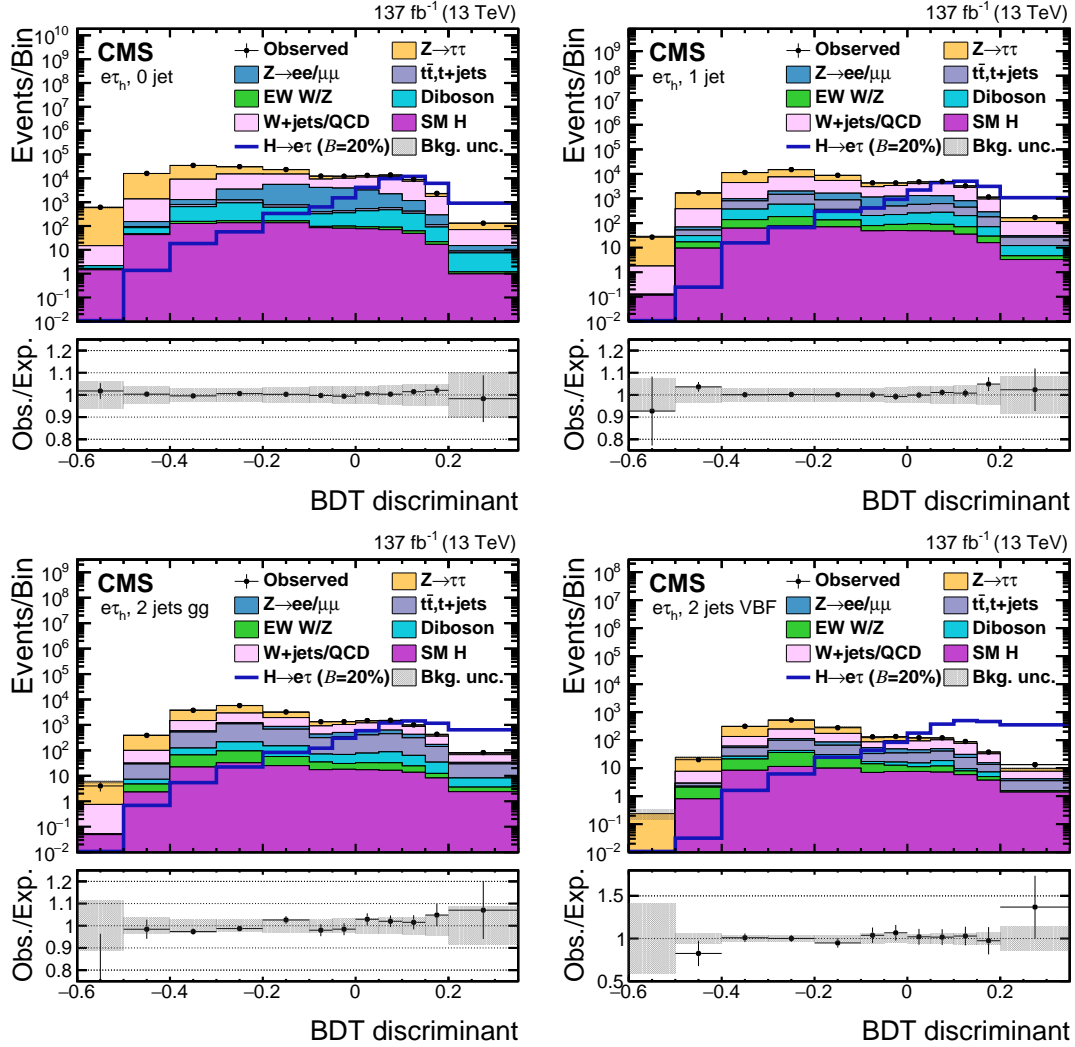


Figure 4: BDT discriminant distributions for the data and background processes in the $H \rightarrow e\tau_h$ channel. A $\mathcal{B}(H \rightarrow e\tau) = 20\%$ is assumed for the signal. The channel categories are 0 jets (upper row left), 1 jet (upper row right), 2 jets ggH (lower row left), and 2 jets VBF (lower row right). The lower panel in each plot shows the ratio of data and estimated background. The uncertainty band corresponds to the background uncertainty in which the post-fit statistical and systematic uncertainties are added in quadrature.

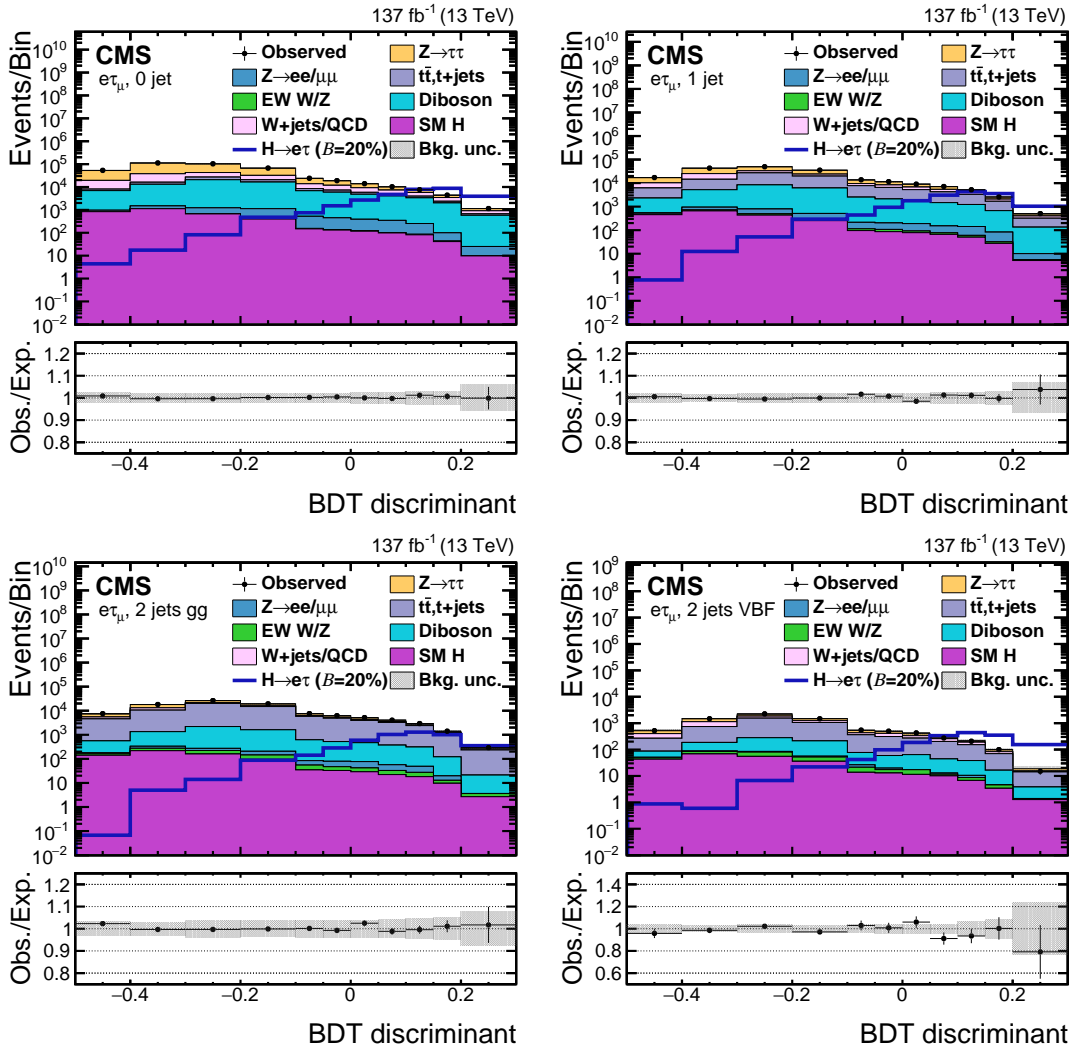


Figure 5: BDT discriminant distributions for the data and background processes in the $H \rightarrow e\tau_\mu$ channel. A $\mathcal{B}(H \rightarrow e\tau) = 20\%$ is assumed for the signal. The channel categories are 0 jets (upper row left), 1 jet (upper row right), 2 jets ggH (lower row left), and 2 jets VBF (lower row right). The lower panel in each plot shows the ratio of data and estimated background. The uncertainty band corresponds to the background uncertainty in which the post-fit statistical and systematic uncertainties are added in quadrature.

$t\bar{t}$, diboson, and EW W/Z events. The simulated events from the $t\bar{t}$, diboson, and EW W/Z where both τ candidates match to τ leptons at the generator level are removed to avoid any double counting.

6.2 Misidentified lepton background

The misidentified lepton background corresponds to events where jets are misidentified as leptons. They mostly arise from two sources: W+jets and QCD multijet events. In W+jets background events, one of the leptons is from the W boson decay while the other is a jet misidentified as a lepton. In QCD multijet events, both the leptons are misidentified jets. In the $\mu\tau_h$ and $e\tau_h$ channels, the contributions from misidentified lepton backgrounds have been estimated using a “misidentification rate” approach. In the $\mu\tau_e$ and $e\tau_\mu$ channels, an “extrapolation factor” approach is adopted, which is consistent with the “misidentification rate” approach, and is used because of limited statistical precision in the leptonic channels.

6.2.1 Misidentification rate approach

The misidentified lepton background in the signal region (SR) is estimated using misidentification rates from Z+jets CR and applied to a background-enriched region from collision data. The misidentification rates are evaluated using events with a Z boson and at least one jet that can be misidentified as a lepton. The probabilities with which jets are misidentified as an electron, muon, or τ_h are labeled as $f_e, f_\mu,$ and f_{τ_h} , respectively. The Z boson is formed using two muons with $p_T > 26$ GeV, $|\eta| < 2.4$, and $I_{\text{rel}}^\mu < 0.15$ for measuring the jet $\rightarrow \tau_h, \mu, e$ misidentification rate. The muons are required to be oppositely charged and have invariant mass between 70 and 110 GeV. The contribution from diboson events, where there is a genuine lepton, is subtracted using simulation.

The jet is required to pass the same lepton identification criteria as used in the SR. A “signal-like” and “background-like” regions are defined. The isolation for the electron and muon is required to have $I_{\text{rel}}^\ell < 0.15$ and the τ_h discriminated against jets at a WP that has an identification efficiency of about 70% for the “signal-like” region. For the “background-like” region, lepton isolation is required to be $0.15 < I_{\text{rel}}^\mu < 0.25$ and $0.15 < I_{\text{rel}}^e < 0.50$, and the τ_h is discriminated against jets at a WP that has an identification efficiency of about 80% and not pass the WP that has an identification efficiency of about 70%. After the “signal-like” and “background-like” regions are defined, the misidentification rates are computed as functions of the lepton p_T . The misidentification rates $f_e, f_\mu,$ and f_{τ_h} are estimated as:

$$f_i = \frac{S_i}{B_i + S_i}$$

where S_i is the number of events in the “signal-like” region, while B_i is the number of events in the “background-like” region. The τ_h misidentification rate shows a p_T dependence that depends on the τ_h decay mode and $|\eta|$ and is therefore evaluated as a function of p_T^τ for the different decay modes and two η regions ($|\eta| < 1.5$ or $|\eta| > 1.5$).

In the $e\tau_h$ channel, the τ_h misidentification rate is evaluated using events with a Z boson formed using two electrons with $p_T > 27$ GeV, $|\eta| < 2.5$, and $I_{\text{rel}}^e < 0.15$. The electrons must be oppositely charged and have an invariant mass between 70 and 110 GeV. The reason for using Z $\rightarrow ee$ events for evaluating the τ_h misidentification rate in $e\tau_h$ channel is that the DNN WPs used for discriminating τ_h against electrons and muons are different in this channel compared to the $\mu\tau_h$ channel as described in Section 4. The misidentification rates evaluated using this CR are compatible with the misidentification rates measured in Z $\rightarrow \mu\mu$ events.

The computed misidentification rates f_i depend on the lepton p_T for electrons and muons or p_T , η , and decay mode for the τ_h candidates. The misidentification rates for electrons and muons are ≈ 0.4 and ≈ 0.6 , respectively, at $p_T = 30.0$ GeV. The misidentification rates for τ_h candidates are in the range 0.02–0.24 at $p_T = 30.0$ GeV. They are used to estimate the background yields and obtain the distributions of the misidentified lepton background. This is accomplished through the following procedure. Each event in the “background-like” region, defined using the collision data with the same selection as the SR, but loosening the isolation requirements on one of the leptons, is weighted by a factor $f_i/(1 - f_i)$. Events with the possibility of double counting because of two misidentified leptons are subtracted. For example, events with both a misidentified muon or electron and a misidentified τ_h are accounted once in the “background-like” region for muon or electron with a weight $f_\ell/(1 - f_\ell)$ and another time in the “background-like” region for τ_h with a weight $f_\tau/(1 - f_\tau)$ and are hence double counted. This is mitigated by subtracting their contribution once using a weight, $f_\tau f_\ell / [(1 - f_\tau)(1 - f_\ell)]$, where $\ell = \mu$ or e .

The background estimate is validated in a VR by requiring the two leptons to have the same electric charge, enhancing the misidentified lepton background. Figure 6 (left) shows the comparison of data with background estimates in this VR for the $\mu\tau_h$ channel. The background estimate is also validated in a W boson enriched VR, as shown in Fig. 6 (middle). This VR is obtained by applying the preselection, $m_T(\ell, \vec{p}_T^{\text{miss}}) > 60$ GeV ($\ell = e$ or μ), and $m_T(\tau_h, \vec{p}_T^{\text{miss}}) > 80$ GeV.

6.2.2 Extrapolation factor approach

In the $e\tau_\mu$ and $\mu\tau_e$ channels, the QCD multijet background is estimated from the data using events with an electron and a muon with the same electric charge [77]. Contributions from other processes are estimated from simulation and subtracted from the data. Extrapolation factors from the CR requiring the two leptons to have the same electric charge to the SR are measured in data as a function of the jet multiplicity and the ΔR separation between the electron and muon.

The extrapolation factors are estimated using events with a muon failing the isolation requirement and an isolated electron. The contribution from $b\bar{b}$ events to the QCD multijet background gives rise to the ΔR dependence and is parameterized with a linear function. The extrapolation factors are higher for events with low ΔR separation between the electron and muon, decreasing as the ΔR separation increases. The extrapolation factors also depend on the electron and muon p_T . This p_T dependence comes from the leptons arising from the semi-leptonic c quark decay. These leptons tend to be softer in p_T and less isolated, resulting in a reduction in the number of such events passing the p_T and isolation requirements.

As the extrapolation factors are from CR where the muon fails the isolation requirement, an additional correction is applied to cover a potential mismodeling. This correction is calculated by measuring the extrapolation factors in two different CRs. The first CR has events where the muon is isolated, and the electron fails the isolation requirement. The second CR has events where both the electron and muon fail the isolation requirement. The ratio of the extrapolation factors from these two CRs is taken as the correction to account for the potential mismodeling induced by requiring the muon to fail the isolation requirement.

6.3 Other backgrounds

Other background contributions come from processes in which a lepton pair is produced from the weak decays of quarks and vector bosons. These include $t\bar{t}$, WW , WZ , and ZZ events.

There are nonnegligible contributions from processes such as $W\gamma^{(*)}+\text{jets}$, single top quark production, and $Z \rightarrow \ell\ell$ ($\ell = e, \mu$). Figure 6 (right) shows the comparison of data with background estimates in the $t\bar{t}$ VR for the $\mu\tau_e$ channel. This VR is defined by requiring the presence of at least one b-tagged jet in the event in addition to the preselection. The SM Higgs boson production contribution mainly comes from $H \rightarrow \tau\tau$ and $H \rightarrow WW$ decays.

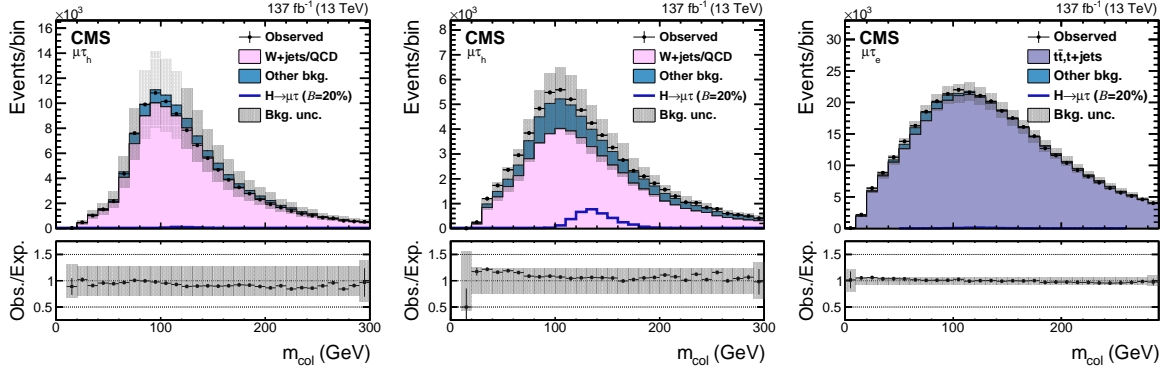


Figure 6: The m_{col} distribution in VR with same electric charge for both leptons (left), $W+\text{jets}$ VR (middle), and $t\bar{t}$ VR (right). In each distribution, the VR’s dominant background is shown, and all the other backgrounds are grouped into “Other bkg.”. A $\mathcal{B}(H \rightarrow \mu\tau) = 20\%$ is assumed for the signal. The lower panel in each plot shows the ratio of data and estimated background. The uncertainty band corresponds to the background uncertainty in which the post-fit statistical and systematic uncertainties are added in quadrature.

7 Systematic uncertainties

Several sources of experimental and theoretical systematic uncertainties are taken into account in the statistical analysis. These uncertainties affect both the normalization and distribution of the different processes. The different systematic uncertainties are incorporated in the likelihood as nuisance parameters for which log-normal a priori distributions are assumed, and distribution variations are taken into account via continuous morphing [78]. The maximum likelihood and profile likelihood with asymptotic approximation are then computed using the defined likelihood to obtain the best fit branching fraction and upper limits on the branching fraction for the LFV Higgs boson decays. As the search is categorized into different final states, partial and complete correlations between the uncertainties in different categories are taken into account and are summarized in Table 3.

The uncertainties to reconstruct a τ_h and estimate its identification efficiency for different p_T ranges are measured using a tag-and-probe method [79] and found to be in the range of 2–3%. The uncertainties for different ranges of p_T are treated as uncorrelated. These uncertainties are also considered for the embedded $\tau\tau$ background, where they are treated as 50% correlated with the simulation uncertainties. For the embedded events, triggering on muons before being replaced by τ leptons leads to an uncertainty in the trigger efficiency of about 4%, which is treated as uncorrelated between the three years due to different triggering criteria. There are two effects that need to be considered for the embedded events. The embedded events have higher track reconstruction efficiency because of reconstruction in an empty detector environment. The energy deposits of the replaced muons can cause event migration for τ_h decay modes with a π^0 . Data to simulation scale factors cover these effects with corresponding systematic uncertainties.

Uncertainties arising from an electron or a muon misidentified as τ_h correspond to between 7–40% or 10–70%, respectively, for different bins of p_T , η , and τ_h decay modes. The uncertainty in the τ_h energy scale is treated as uncorrelated for different decay modes and 50% correlated between embedded and simulated backgrounds and ranges from 0.7–1.2%. The uncertainty in the electron energy scale and the muon momentum scale for misidentified leptons is independent of the τ_h energy scale and amounts to 7% and 1%, respectively. The effect of lepton energy resolution is found to be negligible.

The jet energy scale is affected by several sources, and its uncertainty is evaluated as a function of p_T and η . The jet energy scale's effect is propagated to the BDT discriminant and varies from 3–20% [72]. The uncertainties in jet energy resolution are also taken into account and mostly impact the m_{jj} -defined categories. The jets with $p_T < 10$ GeV fall under unclustered energy. The unclustered energy scale is considered independently for charged particles, neutral hadrons, photons, and very forward particles, that affect both the distributions and the total yields and are treated as uncorrelated. The efficiency to classify a jet as b-tagged is different in data and simulation, and scale factors that depend on jet p_T are used to correct the simulation. The uncertainties in the measured values of these scale factors are taken as sources of systematic uncertainties.

The uncertainties in the reconstruction of electrons and muons, along with their isolation criteria, are measured using the tag-and-probe method in data in $Z \rightarrow ee$ and $Z \rightarrow \mu\mu$ events and sum up to about 2% [64, 80, 81]. The uncertainty in the measurement of the muon momentum scale is in the range 0.4–2.7% for different $|\eta|$ ranges, while for the electron momentum scale, it is less than 1%. The selection of events using electron- and muon-based triggers results in an additional 2% uncertainty in the yield of simulated processes. In the $e\tau_h$ channel, an additional 5% uncertainty is associated with using the trigger requiring the presence of both an electron and τ_h in 2017 and 2018. The uncertainties related to the lepton identification and momentum scale are treated as correlated between the three years, while the uncertainties related to the triggering are treated as uncorrelated.

The misidentification rates in the $e\tau_h$ and $\mu\tau_h$ final states are parameterized using a linear function dependent on $\tau_h p_T$, where two uncertainties are ascribed per fit function. The normalization uncertainties in the estimates of the misidentified lepton backgrounds ($\text{jet} \rightarrow \tau_h, \mu, e$) from data are taken from the VR, which is defined orthogonally to the SR. Additional uncertainty is estimated for the misidentified lepton background in the W boson enriched VR. It is parameterized as a function of $\Delta\phi(\mu, \vec{p}_T^{\text{miss}})$ for the $\mu\tau_h$ channel and as a function of $\Delta\phi(e, \vec{p}_T^{\text{miss}})$ for the $e\tau_h$ channel. Discriminants with different signal-to-background ratios are used to differentiate τ_h against electrons and muons, which entails an additional 3% uncertainty for the $e\tau_h$ channel.

The misidentified lepton background in the $e\tau_\mu$ and $\mu\tau_e$ final states is affected by different uncertainties. The statistical uncertainties arising from both fits of the extrapolation factors as a function of the lepton p_T and the spatial separation between electron and muon are taken into account. The uncertainty in extrapolation factors resulting from inverting the muon isolation is taken into account. These uncertainties have a combined effect of about 20% on the normalization. The dominant source of uncertainty in the simulated background processes, $Z \rightarrow ee$, $Z \rightarrow \mu\mu$, $Z \rightarrow \tau\tau$, WW , ZZ , $W\gamma$, $t\bar{t}$, and single top quark production is the measurement of the cross section for these processes and is treated as correlated between the three years.

The theoretical uncertainties affecting the measurement of Higgs boson production cross section are the QCD scales (renormalization and factorization scales), the choice of PDFs, and the strong coupling constant (α_s) evaluated at the Z boson mass. These uncertainties affect the

signal's normalization and are treated as correlated between the three years [82]. The changes made in QCD scales provide 3.9, 0.5, 0.9, and 0.8% uncertainties in the ggH, VBF, ZH, WH cross sections, respectively, while changes in the PDFs and α_s result in 3.2, 2.1, 1.3, and 1.9% uncertainties, respectively. The acceptance is taken into account when changes are made in QCD scales and the PDFs and α_s .

The normalization of the event yield for $H \rightarrow \tau\tau$ is taken from simulation. The uncertainty in the $\mathcal{B}(H \rightarrow \tau\tau)$ includes a 1.70% due to missing higher-order corrections, a 0.99% in the quark masses, and a 0.62% on α_s . The normalization of the event yield for $H \rightarrow WW$ is taken from simulation. The uncertainty in the $\mathcal{B}(H \rightarrow WW)$ includes a 0.99% due to missing higher-order corrections, a 0.99% in the quark masses, and a 0.66% in α_s .

The bin-by-bin uncertainties account for the statistical uncertainties in each bin of the distributions of every process. The Barlow–Beeston Lite [83] approach is used, assigning a single parameter to scale the sum of the process yields in each bin, constrained by the total uncertainty, instead of requiring separate parameters, one per process. This is useful to reduce the number of parameters required in the statistical analysis. They are treated as uncorrelated between bins, categories, and channels.

The integrated luminosities of the 2016, 2017, and 2018 data taking periods are individually known to have uncertainties in the 2.3–2.5% range [84–86], while the total integrated luminosity has an uncertainty of 1.8%, the improvement in precision reflecting the uncorrelated time evolution of some systematic effects. The uncertainty in the integrated luminosity affects all processes, with the normalization taken directly from the simulation. Uncertainty related to pileup is evaluated through changes made in the weights applied to the simulation and is treated as correlated between the three years. The dependence on weight is obtained through a 5% change in the total inelastic cross section used to estimate the number of pileup events in data. Other minimum-bias event modeling and initial- and final-state radiation uncertainties are estimated to be much smaller than those on the rate and are therefore neglected.

During the 2016 and 2017 data taking periods, a gradual shift in the timing of the inputs from the ECAL first-level trigger in the region of $|\eta| > 2.0$ caused a specific trigger inefficiency. For events containing an electron or a jet with respective $p_T > 50$ GeV or > 100 GeV, in the region $2.5 < |\eta| < 3.0$ the efficiency loss is 10–20%, depending on p_T , η , and time. Correction factors are computed from data and applied to the acceptance evaluated through simulation. Uncertainty due to this correction factor is $\approx 1\%$ and is treated as correlated between the two years.

8 Results

No significant excess has been found for the LFV Higgs boson decays in both channels, and upper limits have been placed. Upper limits on the branching fraction of Higgs boson decay are computed using the modified frequentist approach for CL_s , taking the profile likelihood as a test statistic [87–89] in the asymptotic approximation. The observed (expected) upper limits on the Higgs boson branching fractions are 0.15 (0.15)% for $H \rightarrow \mu\tau$ and 0.22 (0.16)% for $H \rightarrow e\tau$, respectively, at the 95% CL. The results have a dominant contribution from systematic uncertainties. The bin-by-bin uncertainties and the uncertainties related to the distribution of the misidentified lepton background have a significant impact followed by the lepton energy scale uncertainties.

The upper limits and the best fit branching fractions for $\mathcal{B}(H \rightarrow \mu\tau)$ and $\mathcal{B}(H \rightarrow e\tau)$ are

Table 3: Systematic uncertainties in the expected event yields. All uncertainties are treated as correlated among categories, except those with two values separated by the \oplus sign. In this case, the first value is the correlated uncertainty and the second value is the uncorrelated uncertainty for each category.

| Systematic uncertainty | $\mu\tau_h$ | $\mu\tau_e$ | $e\tau_h$ | $e\tau_\mu$ |
|---------------------------------------|-------------------|----------------|--------------------|----------------|
| Muon ident. and iso. | 2% | 2% | — | 2% |
| Electron ident. and iso. | — | 2% | 2% | 2% |
| Trigger | 2% | 2% | 2% | 2% |
| τ_h ident. | p_T dep. (2–3%) | — | p_T dep. (2–15%) | — |
| $\mu \rightarrow \tau_h$ misid. | 10–70% | — | — | — |
| $e \rightarrow \tau_h$ misid. | — | — | 40% | — |
| b tagging efficiency | <6.5% | <6.5% | <6.5% | <6.5% |
| Embedded bkg. | 4% | 4% | 4% | 4% |
| $Z \rightarrow \mu\mu, ee$ bkg. | 4% \oplus 5% | 4% \oplus 5% | 4% \oplus 5% | 4% \oplus 5% |
| EW bkg. | 4% \oplus 5% | 4% \oplus 5% | 4% \oplus 5% | 4% \oplus 5% |
| W +jets bkg. | — | 10% | — | 10% |
| Diboson bkg. | 5% \oplus 5% | 5% \oplus 5% | 5% \oplus 5% | 5% \oplus 5% |
| $t\bar{t}$ bkg. | 6% \oplus 5% | 6% \oplus 5% | 6% \oplus 5% | 6% \oplus 5% |
| Single top quark bkg. | 5% \oplus 5% | 5% \oplus 5% | 5% \oplus 5% | 5% \oplus 5% |
| $\text{Jet} \rightarrow \tau_h$ bkg. | 30% \oplus 10% | — | 30% \oplus 10% | — |
| Jet energy scale | 3–20% | 3–20% | 3–20% | 3–20% |
| τ_h energy scale | 0.7–1.2% | — | 0.7–1.2% | — |
| $e \rightarrow \tau_h$ energy scale | 1–7% | — | 1–7% | — |
| $\mu \rightarrow \tau_h$ energy scale | 1% | — | 1% | — |
| Electron energy scale | — | 1–2.5% | 1–2.5% | 1–2.5% |
| Muon energy scale | 0.4–2.7% | 0.4–2.7% | — | 0.4–2.7% |
| Trigger timing inefficiency | 0.2–1.3% | 0.2–1.3% | 0.2–1.3% | 0.2–1.3% |
| Integrated luminosity | 1.8% | 1.8% | 1.8% | 1.8% |
| QCD scales (ggH) | | 3.9% | | |
| QCD scales (VBF) | | 0.5% | | |
| PDF + α_S (ggH) | | 3.2% | | |
| PDF + α_S (VBF) | | 2.1% | | |
| QCD acceptance (ggH) | | –10.3 to +5.9% | | |
| QCD acceptance (VBF) | | –2.7 to +2.3% | | |
| PDF + α_S acceptance (ggH) | | –0.8 to +2.8% | | |
| PDF + α_S acceptance (VBF) | | –1.7 to +2.3% | | |

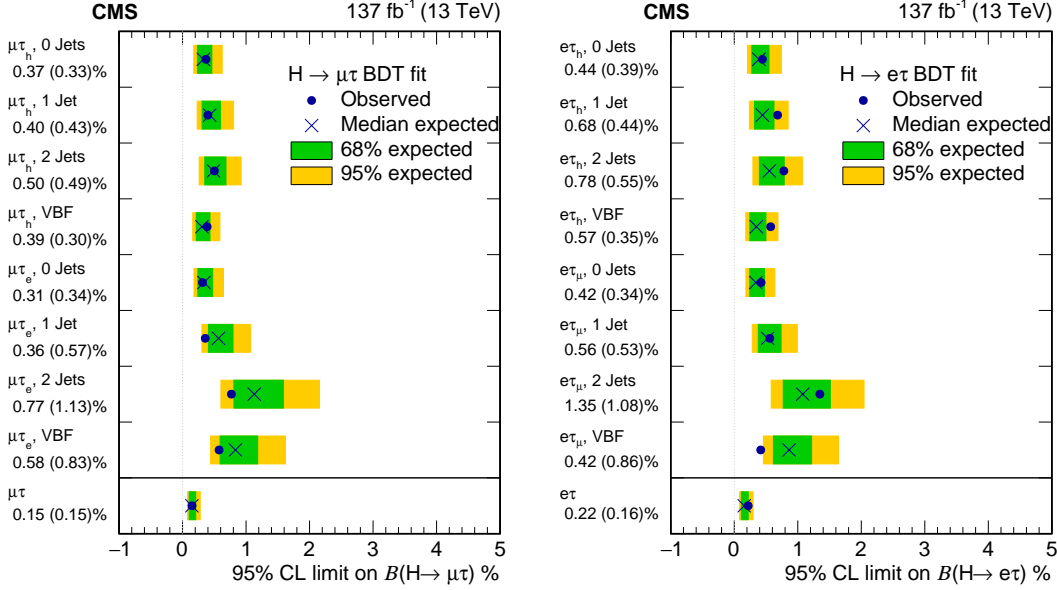


Figure 7: Observed (expected) 95% CL upper limits on the $\mathcal{B}(H \rightarrow \mu\tau)$ (left) and $\mathcal{B}(H \rightarrow e\tau)$ (right) for each individual category and combined. The categories from top to bottom row are $\mu\tau_h$ 0Jets, $\mu\tau_h$ 1Jet, $\mu\tau_h$ 2 Jets, $\mu\tau_h$ VBF, $\mu\tau_e$ 0Jets, $\mu\tau_e$ 1Jet, $\mu\tau_e$ 2 Jets, $\mu\tau_e$ VBF, and $\mu\tau$ combined (left) and $e\tau_h$ 0Jets, $e\tau_h$ 1Jet, $e\tau_h$ 2 Jets, $e\tau_h$ VBF, $e\tau_\mu$ 0Jets, $e\tau_\mu$ 1Jet, $e\tau_\mu$ 2 Jets, $e\tau_\mu$ VBF, and $e\tau$ combined (right).

reported in Tables 4 and 5. The limits are also summarized in Table 6 and graphically shown in Fig. 7. The limits are improved from previous results [30]. The improvement relies on the larger data set, the updated background estimation techniques, and BDT classification. The results are cross-checked with an additional investigation following the strategy in Ref. [30] and are found to be consistent.

The upper limits on $\mathcal{B}(H \rightarrow \mu\tau)$ and $\mathcal{B}(H \rightarrow e\tau)$ are subsequently used to put constraints on LFV Yukawa couplings [11]. The LFV decays $e\tau$ and $\mu\tau$ arise at tree level from the assumed flavor violating Yukawa interactions, $Y_{\ell^\alpha \ell^\beta}$, where ℓ^α, ℓ^β are the leptons of different flavors ($\ell^\alpha \neq \ell^\beta$). The decay widths $\Gamma(H \rightarrow \ell^\alpha \ell^\beta)$ in terms of the Yukawa couplings are given by:

$$\Gamma(H \rightarrow \ell^\alpha \ell^\beta) = \frac{m_H}{8\pi} (|Y_{\ell^\alpha \ell^\beta}|^2 + |Y_{\ell^\beta \ell^\alpha}|^2),$$

and the branching fractions are given by:

$$\mathcal{B}(H \rightarrow \ell^\alpha \ell^\beta) = \frac{\Gamma(H \rightarrow \ell^\alpha \ell^\beta)}{\Gamma(H \rightarrow \ell^\alpha \ell^\beta) + \Gamma_{\text{SM}}}.$$

The SM Higgs boson decay width is assumed to be $\Gamma_{\text{SM}} = 4.1 \text{ MeV}$ [90] for $m_H = 125 \text{ GeV}$. The 95% CL upper limit on the Yukawa couplings obtained from the expression for the branching fraction above is shown in Table 6. The limits on the Yukawa couplings are $\sqrt{|Y_{\mu\tau}|^2 + |Y_{\tau\mu}|^2} < 1.11 \times 10^{-3}$ and $\sqrt{|Y_{e\tau}|^2 + |Y_{\tau e}|^2} < 1.35 \times 10^{-3}$ and are shown in Fig. 8. Tabulated results are available in the HepData database [91].

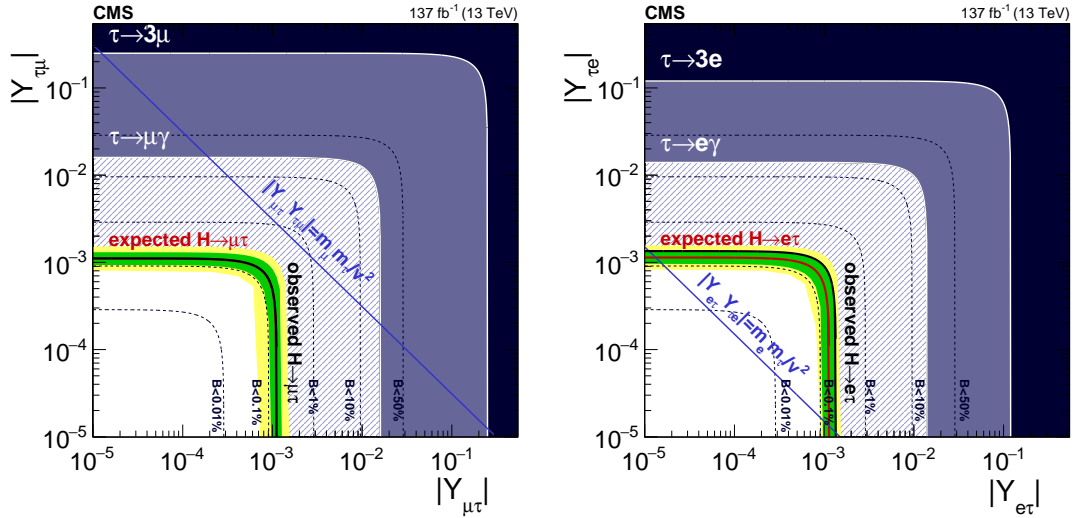


Figure 8: Expected (red line) and observed (black solid line) 95% CL upper limits on the LFV Yukawa couplings, $|Y_{\mu\tau}|$ vs. $|Y_{\tau\mu}|$ (left) and $|Y_{e\tau}|$ vs. $|Y_{\tau e}|$ (right). The $|Y_{\mu\tau}|$ or $|Y_{e\tau}|$ couplings correspond to left chiral muon or electron and right chiral τ lepton, while $|Y_{\tau\mu}|$ or $|Y_{\tau e}|$ couplings correspond to left chiral τ lepton and right chiral muon or electron. In the left plot, the expected limit is covered by the observed limit as they have similar values. The flavor diagonal Yukawa couplings are approximated by their SM values. The green and yellow bands indicate the range that is expected to contain 68% and 95% of all observed limit variations from the expected limit. The shaded regions are constraints obtained from null searches for $\tau \rightarrow 3\mu$ or $\tau \rightarrow 3e$ (dark blue) [92] and $\tau \rightarrow \mu\gamma$ or $\tau \rightarrow e\gamma$ (purple) [93]. The blue diagonal line is the theoretical naturalness limit $|Y_{ij}Y_{ji}| = m_i m_j / v^2$ [11].

Table 4: Observed and expected upper limits at 95% CL and best fit branching fractions for each individual jet category, and their combinations, in the $H \rightarrow \mu\tau$ channel.

| | | Expected limits (%) | | | | |
|-------------|--|----------------------------------|------------------|------------------|------------------|------------------|
| | | 0-jet | 1-jet | 2-jets | VBF | Combined |
| $\mu\tau_e$ | | <0.34 | <0.57 | <1.13 | <0.83 | <0.27 |
| $\mu\tau_h$ | | <0.33 | <0.43 | <0.49 | <0.30 | <0.18 |
| $\mu\tau$ | | | | | | <0.15 |
| | | Observed limits (%) | | | | |
| | | 0-jet | 1-jet | 2-jets | VBF | Combined |
| $\mu\tau_e$ | | <0.31 | <0.36 | <0.77 | <0.58 | <0.19 |
| $\mu\tau_h$ | | <0.37 | <0.40 | <0.50 | <0.39 | <0.24 |
| $\mu\tau$ | | | | | | <0.15 |
| | | Best fit branching fractions (%) | | | | |
| | | 0-jet | 1-jet | 2-jets | VBF | Combined |
| $\mu\tau_e$ | | -0.03 ± 0.17 | -0.40 ± 0.28 | -0.66 ± 0.56 | -0.41 ± 0.39 | -0.14 ± 0.13 |
| $\mu\tau_h$ | | $+0.05 \pm 0.17$ | -0.05 ± 0.22 | $+0.02 \pm 0.25$ | $+0.10 \pm 0.16$ | $+0.07 \pm 0.09$ |
| $\mu\tau$ | | | | | | $+0.00 \pm 0.07$ |

Table 5: Observed and expected upper limits at 95% CL and best fit branching fractions for each individual jet category, and their combinations, in the $H \rightarrow e\tau$ channel.

| | Expected limits (%) | | | | |
|-------------|----------------------------------|------------------|------------------|------------------|------------------|
| | 0-jet | 1-jet | 2-jets | VBF | Combined |
| $e\tau_\mu$ | <0.34 | <0.53 | <1.08 | <0.86 | <0.26 |
| $e\tau_h$ | <0.39 | <0.44 | <0.55 | <0.35 | <0.20 |
| $e\tau$ | | | | | <0.16 |
| | Observed limits (%) | | | | |
| | 0-jet | 1-jet | 2-jets | VBF | Combined |
| $e\tau_\mu$ | <0.42 | <0.56 | <1.35 | <0.42 | <0.22 |
| $e\tau_h$ | <0.44 | <0.68 | <0.78 | <0.57 | <0.37 |
| $e\tau$ | | | | | <0.22 |
| | Best fit branching fractions (%) | | | | |
| | 0-jet | 1-jet | 2-jets | VBF | Combined |
| $e\tau_\mu$ | $+0.11 \pm 0.17$ | $+0.04 \pm 0.27$ | $+0.35 \pm 0.55$ | -1.04 ± 0.44 | -0.07 ± 0.13 |
| $e\tau_h$ | $+0.07 \pm 0.20$ | $+0.29 \pm 0.23$ | $+0.27 \pm 0.29$ | $+0.27 \pm 0.17$ | $+0.20 \pm 0.10$ |
| $e\tau$ | | | | | $+0.08 \pm 0.08$ |

Table 6: Summary of observed and expected upper limits at 95% CL, best fit branching fractions and corresponding constraints on Yukawa couplings for the $H \rightarrow \mu\tau$ and $H \rightarrow e\tau$ channels.

| | Observed (expected) upper limits (%) | Best fit branching fractions (%) | Yukawa coupling constraints |
|-------------------------|-----------------------------------------|-------------------------------------|--------------------------------|
| $H \rightarrow \mu\tau$ | <0.15 (0.15) | 0.00 ± 0.07 | $< 1.11 (1.10) \times 10^{-3}$ |
| $H \rightarrow e\tau$ | <0.22 (0.16) | 0.08 ± 0.08 | $< 1.35 (1.14) \times 10^{-3}$ |

9 Summary

A search for lepton-flavor violation has been performed in the $\mu\tau$ and $e\tau$ final states of the Higgs boson in data collected by the CMS experiment. The data correspond to an integrated luminosity of 137 fb^{-1} of proton-proton collisions at a center-of-mass energy of 13 TeV. The results are extracted through a maximum likelihood fit to a boosted decision tree output, trained to distinguish the expected signal from backgrounds. The observed (expected) upper limits on the branching fraction of the Higgs boson to $\mu\tau$ are 0.15 (0.15)% and to $e\tau$ are 0.22 (0.16)%, respectively, at 95% confidence level. Upper limits on the off-diagonal $\mu\tau$ and $e\tau$ couplings are derived from these constraints, $\sqrt{|Y_{\mu\tau}|^2 + |Y_{\tau\mu}|^2} < 1.11 \times 10^{-3}$ and $\sqrt{|Y_{e\tau}|^2 + |Y_{\tau e}|^2} < 1.35 \times 10^{-3}$. These results constitute an improvement over the previous limits from CMS and ATLAS experiments.

Acknowledgments

We congratulate our colleagues in the CERN accelerator departments for the excellent performance of the LHC and thank the technical and administrative staffs at CERN and at other CMS institutes for their contributions to the success of the CMS effort. In addition, we gratefully acknowledge the computing centers and personnel of the Worldwide LHC Computing Grid and other centers for delivering so effectively the computing infrastructure essential to our analyses. Finally, we acknowledge the enduring support for the construction and operation of the LHC, the CMS detector, and the supporting computing infrastructure provided by the following funding agencies: BMBWF and FWF (Austria); FNRS and FWO (Belgium); CNPq, CAPES, FAPERJ, FAPERGS, and FAPESP (Brazil); MES (Bulgaria); CERN; CAS, MoST, and NSFC (China); MINCIENCIAS (Colombia); MSES and CSF (Croatia); RIF (Cyprus); SENESCYT (Ecuador); MoER, ERC PUT and ERDF (Estonia); Academy of Finland, MEC, and HIP (Finland); CEA and CNRS/IN2P3 (France); BMBF, DFG, and HGF (Germany); GSRT (Greece); NKFI (Hungary); DAE and DST (India); IPM (Iran); SFI (Ireland); INFN (Italy); MSIP and NRF (Republic of Korea); MES (Latvia); LAS (Lithuania); MOE and UM (Malaysia); BUAP, CINVESTAV, CONACYT, LNS, SEP, and UASLP-FAI (Mexico); MOS (Montenegro); MBIE (New Zealand); PAEC (Pakistan); MSHE and NSC (Poland); FCT (Portugal); JINR (Dubna); MON, RosAtom, RAS, RFBR, and NRC KI (Russia); MESTD (Serbia); SEIDI, CPAN, PCTI, and FEDER (Spain); MOSTR (Sri Lanka); Swiss Funding Agencies (Switzerland); MST (Taipei); ThEPCenter, IPST, STAR, and NSTDA (Thailand); TUBITAK and TAEK (Turkey); NASU (Ukraine); STFC (United Kingdom); DOE and NSF (USA).

Individuals have received support from the Marie-Curie program and the European Research Council and Horizon 2020 Grant, contract Nos. 675440, 724704, 752730, 765710 and 824093 (European Union); the Leventis Foundation; the Alfred P. Sloan Foundation; the Alexander von Humboldt Foundation; the Belgian Federal Science Policy Office; the Fonds pour la Formation à la Recherche dans l'Industrie et dans l'Agriculture (FRIA-Belgium); the Agentschap voor Innovatie door Wetenschap en Technologie (IWT-Belgium); the F.R.S.-FNRS and FWO (Belgium) under the "Excellence of Science – EOS" – be.h project n. 30820817; the Beijing Municipal Science & Technology Commission, No. Z191100007219010; the Ministry of Education, Youth and Sports (MEYS) of the Czech Republic; the Deutsche Forschungsgemeinschaft (DFG), under Germany's Excellence Strategy – EXC 2121 "Quantum Universe" – 390833306, and under project number 400140256 - GRK2497; the Lendület ("Momentum") Program and the János Bolyai Research Scholarship of the Hungarian Academy of Sciences, the New National Excellence Program ÚNKP, the NKFI research grants 123842, 123959, 124845, 124850, 125105, 128713, 128786, and 129058 (Hungary); the Council of Science and Industrial Research, In-

dia; the Ministry of Science and Higher Education and the National Science Center, contracts Opus 2014/15/B/ST2/03998 and 2015/19/B/ST2/02861 (Poland); the National Priorities Research Program by Qatar National Research Fund; the Ministry of Science and Higher Education, project no. 0723-2020-0041 (Russia); the Programa Estatal de Fomento de la Investigación Científica y Técnica de Excelencia María de Maeztu, grant MDM-2015-0509 and the Programa Severo Ochoa del Principado de Asturias; the Thalís and Aristeia programs cofinanced by EU-ESF and the Greek NSRF; the Rachadapisek Sompot Fund for Postdoctoral Fellowship, Chulalongkorn University and the Chulalongkorn Academic into Its 2nd Century Project Advancement Project (Thailand); the Kavli Foundation; the Nvidia Corporation; the SuperMicro Corporation; the Welch Foundation, contract C-1845; and the Weston Havens Foundation (USA).

References

- [1] ATLAS Collaboration, “Measurements of the Higgs boson production and decay rates and coupling strengths using pp collision data at $\sqrt{s} = 7$ and 8 TeV in the ATLAS experiment”, *Eur. Phys. J. C* **76** (2016) 6, doi:10.1140/epjc/s10052-015-3769-y, arXiv:1507.04548.
- [2] CMS Collaboration, “Precise determination of the mass of the Higgs boson and tests of compatibility of its couplings with the standard model predictions using proton collisions at 7 and 8 TeV”, *Eur. Phys. J. C* **75** (2015) 212, doi:10.1140/epjc/s10052-015-3351-7, arXiv:1412.8662.
- [3] CMS Collaboration, “Study of the mass and spin-parity of the Higgs boson candidate via its decays to Z boson pairs”, *Phys. Rev. Lett.* **110** (2013) 081803, doi:10.1103/PhysRevLett.110.081803, arXiv:1212.6639.
- [4] ATLAS Collaboration, “Evidence for the spin-0 nature of the Higgs boson using ATLAS data”, *Phys. Lett. B* **726** (2013) 120, doi:10.1016/j.physletb.2013.08.026, arXiv:1307.1432.
- [5] CMS Collaboration, “Constraints on the spin-parity and anomalous HVV couplings of the Higgs boson in proton collisions at 7 and 8 TeV”, *Phys. Rev. D* **92** (2015) 012004, doi:10.1103/PhysRevD.92.012004, arXiv:1411.3441.
- [6] CMS Collaboration, “Measurements of properties of the Higgs boson decaying into the four-lepton final state in pp collisions at $\sqrt{s} = 13$ TeV”, *JHEP* **11** (2017) 047, doi:10.1007/JHEP11(2017)047, arXiv:1706.09936.
- [7] ATLAS Collaboration, “Observation of a new particle in the search for the standard model Higgs boson with the ATLAS detector at the LHC”, *Phys. Lett. B* **716** (2012) 1, doi:10.1016/j.physletb.2012.08.020, arXiv:1207.7214.
- [8] CMS Collaboration, “Observation of a new boson at a mass of 125 GeV with the CMS experiment at the LHC”, *Phys. Lett. B* **716** (2012) 30, doi:10.1016/j.physletb.2012.08.021, arXiv:1207.7235.
- [9] CMS Collaboration, “Observation of a new boson with mass near 125 GeV in pp collisions at $\sqrt{s} = 7$ and 8 TeV”, *JHEP* **06** (2013) 081, doi:10.1007/JHEP06(2013)081, arXiv:1303.4571.

- [10] CMS Collaboration, “Combined measurements of Higgs boson couplings in proton–proton collisions at $\sqrt{s} = 13$ TeV”, *Eur. Phys. J. C* **79** (2019) 421, doi:10.1140/epjc/s10052-019-6909-y, arXiv:1809.10733.
- [11] R. Harnik, J. Kopp, and J. Zupan, “Flavor violating Higgs decays”, *JHEP* **03** (2013) 026, doi:10.1007/JHEP03(2013)026, arXiv:1209.1397.
- [12] J. D. Bjorken and S. Weinberg, “A mechanism for nonconservation of muon number”, *Phys. Rev. Lett.* **38** (1977) 622, doi:10.1103/PhysRevLett.38.622.
- [13] J. L. Diaz-Cruz and J. J. Toscano, “Lepton flavor violating decays of Higgs bosons beyond the standard model”, *Phys. Rev. D* **62** (2000) 116005, doi:10.1103/PhysRevD.62.116005, arXiv:hep-ph/9910233.
- [14] T. Han and D. Marfatia, “ $h \rightarrow \mu\tau$ at hadron colliders”, *Phys. Rev. Lett.* **86** (2001) 1442, doi:10.1103/PhysRevLett.86.1442, arXiv:hep-ph/0008141.
- [15] A. Arhrib, Y. Cheng, and O. C. W. Kong, “Comprehensive analysis on lepton flavor violating Higgs boson to $\mu^\mp\tau^\pm$ decay in supersymmetry without R parity”, *Phys. Rev. D* **87** (2013) 015025, doi:10.1103/PhysRevD.87.015025, arXiv:1210.8241.
- [16] K. Agashe and R. Contino, “Composite Higgs-mediated FCNC”, *Phys. Rev. D* **80** (2009) 075016, doi:10.1103/PhysRevD.80.075016, arXiv:0906.1542.
- [17] A. Azatov, M. Toharia, and L. Zhu, “Higgs mediated FCNC’s in warped extra dimensions”, *Phys. Rev. D* **80** (2009) 035016, doi:10.1103/PhysRevD.80.035016, arXiv:0906.1990.
- [18] H. Ishimori et al., “Non-Abelian discrete symmetries in particle physics”, *Prog. Theor. Phys. Suppl.* **183** (2010) 1, doi:10.1143/PTPS.183.1, arXiv:1003.3552.
- [19] G. Perez and L. Randall, “Natural neutrino masses and mixings from warped geometry”, *JHEP* **01** (2009) 077, doi:10.1088/1126-6708/2009/01/077, arXiv:0805.4652.
- [20] S. Casagrande et al., “Flavor physics in the Randall-Sundrum model: I. Theoretical setup and electroweak precision tests”, *JHEP* **10** (2008) 094, doi:10.1088/1126-6708/2008/10/094, arXiv:0807.4937.
- [21] A. J. Buras, B. Duling, and S. Gori, “The impact of Kaluza-Klein fermions on standard model fermion couplings in a RS model with custodial protection”, *JHEP* **09** (2009) 076, doi:10.1088/1126-6708/2009/09/076, arXiv:0905.2318.
- [22] M. Blanke et al., “ $\Delta F = 2$ observables and fine-tuning in a warped extra dimension with custodial protection”, *JHEP* **03** (2009) 001, doi:10.1088/1126-6708/2009/03/001, arXiv:0809.1073.
- [23] M. E. Albrecht et al., “Electroweak and flavour structure of a warped extra dimension with custodial protection”, *JHEP* **09** (2009) 064, doi:10.1088/1126-6708/2009/09/064, arXiv:0903.2415.
- [24] G. F. Giudice and O. Lebedev, “Higgs-dependent Yukawa couplings”, *Phys. Lett. B* **665** (2008) 79, doi:10.1016/j.physletb.2008.05.062, arXiv:0804.1753.
- [25] J. A. Aguilar Saavedra, “A minimal set of top-Higgs anomalous couplings”, *Nucl. Phys. B* **821** (2009) 215, doi:10.1016/j.nuclphysb.2009.06.022, arXiv:0904.2387.

-
- [26] A. Goudelis, O. Lebedev, and J. h. Park, “Higgs-induced lepton flavor violation”, *Phys. Lett. B* **707** (2012) 369, doi:10.1016/j.physletb.2011.12.059, arXiv:1111.1715.
- [27] D. McKeen, M. Pospelov, and A. Ritz, “Modified Higgs branching ratios versus CP and lepton flavor violation”, *Phys. Rev. D* **86** (2012) 113004, doi:10.1103/PhysRevD.86.113004, arXiv:1208.4597.
- [28] A. Pilaftsis, “Lepton flavor nonconservation in H^0 decays”, *Phys. Lett. B* **285** (1992) 68, doi:10.1016/0370-2693(92)91301-0.
- [29] J. G. Körner, A. Pilaftsis, and K. Schilcher, “Leptonic CP asymmetries in flavor changing H^0 decays”, *Phys. Rev. D* **47** (1993) 1080, doi:10.1103/PhysRevD.47.1080, arXiv:hep-ph/9301289.
- [30] CMS Collaboration, “Search for lepton flavour violating decays of the Higgs boson to $\mu\tau$ and $e\tau$ in proton-proton collisions at $\sqrt{s} = 13$ TeV”, *JHEP* **06** (2018) 001, doi:10.1007/JHEP06(2018)001, arXiv:1712.07173.
- [31] ATLAS Collaboration, “Searches for lepton-flavour-violating decays of the Higgs boson in $\sqrt{s} = 13$ TeV pp collisions with the ATLAS detector”, *Phys. Lett. B* **800** (2020) 135069, doi:10.1016/j.physletb.2019.135069, arXiv:1907.06131.
- [32] O. U. Shanker, “Flavor violation, scalar particles and leptoquarks”, *Nucl. Phys. B* **206** (1982) 253, doi:10.1016/0550-3213(82)90534-X.
- [33] B. McWilliams and L.-F. Li, “Virtual effects of Higgs particles”, *Nucl. Phys. B* **179** (1981) 62, doi:10.1016/0550-3213(81)90249-2.
- [34] G. Blankenburg, J. Ellis, and G. Isidori, “Flavour-changing decays of a 125 GeV Higgs-like particle”, *Phys. Lett. B* **712** (2012) 386, doi:10.1016/j.physletb.2012.05.007, arXiv:1202.5704.
- [35] MEG Collaboration, “New constraint on the existence of the $\mu^+ \rightarrow e^+ \gamma$ decay”, *Phys. Rev. Lett.* **110** (2013) 201801, doi:10.1103/PhysRevLett.110.201801, arXiv:1303.0754.
- [36] A. Celis, V. Cirigliano, and E. Passemar, “Lepton flavor violation in the Higgs sector and the role of hadronic τ -lepton decays”, *Phys. Rev. D* **89** (2014) 013008, doi:10.1103/PhysRevD.89.013008, arXiv:1309.3564.
- [37] CMS Collaboration, “Search for lepton flavour violating decays of the Higgs boson to $e\tau$ and $e\mu$ in proton-proton collisions at $\sqrt{s} = 8$ TeV”, *Phys. Lett. B* **763** (2016) 472, doi:10.1016/j.physletb.2016.09.062, arXiv:1607.03561.
- [38] CMS Collaboration, “Performance of the CMS Level-1 trigger in proton-proton collisions at $\sqrt{s} = 13$ TeV”, *JINST* **15** (2020) P10017, doi:10.1088/1748-0221/15/10/P10017, arXiv:2006.10165.
- [39] CMS Collaboration, “The CMS trigger system”, *JINST* **12** (2017) P01020, doi:10.1088/1748-0221/12/01/P01020, arXiv:1609.02366.
- [40] CMS Collaboration, “The CMS experiment at the CERN LHC”, *JINST* **3** (2008) S08004, doi:10.1088/1748-0221/3/08/S08004.

- [41] T. Sjöstrand et al., “An introduction to PYTHIA 8.2”, *Comput. Phys. Commun.* **191** (2015) 159, doi:10.1016/j.cpc.2015.01.024, arXiv:1410.3012.
- [42] CMS Collaboration, “Event generator tunes obtained from underlying event and multiparton scattering measurements”, *Eur. Phys. J. C* **76** (2016) 155, doi:10.1140/epjc/s10052-016-3988-x, arXiv:1512.00815.
- [43] CMS Collaboration, “Extraction and validation of a new set of CMS PYTHIA8 tunes from underlying-event measurements”, *Eur. Phys. J. C* **80** (2020) 4, doi:10.1140/epjc/s10052-019-7499-4, arXiv:1903.12179.
- [44] NNPDF Collaboration, “Parton distributions from high-precision collider data”, *Eur. Phys. J. C* **77** (2017) 663, doi:10.1140/epjc/s10052-017-5199-5, arXiv:1706.00428.
- [45] GEANT4 Collaboration, “GEANT4 — a simulation toolkit”, *Nucl. Instrum. Meth. A* **506** (2003) 250, doi:10.1016/S0168-9002(03)01368-8.
- [46] H. M. Georgi, S. L. Glashow, M. E. Machacek, and D. V. Nanopoulos, “Higgs bosons from two gluon annihilation in proton-proton collisions”, *Phys. Rev. Lett.* **40** (1978) 692, doi:10.1103/PhysRevLett.40.692.
- [47] R. N. Cahn, S. D. Ellis, R. Kleiss, and W. J. Stirling, “Transverse momentum signatures for heavy Higgs bosons”, *Phys. Rev. D* **35** (1987) 1626, doi:10.1103/PhysRevD.35.1626.
- [48] S. L. Glashow, D. V. Nanopoulos, and A. Yildiz, “Associated production of Higgs bosons and Z particles”, *Phys. Rev. D* **18** (1978) 1724, doi:10.1103/PhysRevD.18.1724.
- [49] P. Nason, “A new method for combining NLO QCD with shower monte carlo algorithms”, *JHEP* **11** (2004) 040, doi:10.1088/1126-6708/2004/11/040, arXiv:hep-ph/0409146.
- [50] S. Frixione, P. Nason, and C. Oleari, “Matching NLO QCD computations with parton shower simulations: the POWHEG method”, *JHEP* **11** (2007) 070, doi:10.1088/1126-6708/2007/11/070, arXiv:0709.2092.
- [51] S. Alioli, P. Nason, C. Oleari, and E. Re, “A general framework for implementing NLO calculations in shower monte carlo programs: the POWHEG BOX”, *JHEP* **06** (2010) 043, doi:10.1007/JHEP06(2010)043, arXiv:1002.2581.
- [52] S. Alioli et al., “Jet pair production in POWHEG”, *JHEP* **04** (2011) 081, doi:10.1007/JHEP04(2011)081, arXiv:1012.3380.
- [53] S. Alioli, P. Nason, C. Oleari, and E. Re, “NLO Higgs boson production via gluon fusion matched with shower in POWHEG”, *JHEP* **04** (2009) 002, doi:10.1088/1126-6708/2009/04/002, arXiv:0812.0578.
- [54] E. Bagnaschi, G. Degrossi, P. Slavich, and A. Vicini, “Higgs production via gluon fusion in the POWHEG approach in the SM and in the MSSM”, *JHEP* **02** (2012) 088, doi:10.1007/JHEP02(2012)088, arXiv:1111.2854.
- [55] G. Heinrich et al., “NLO predictions for Higgs boson pair production with full top quark mass dependence matched to parton showers”, *JHEP* **08** (2017) 088, doi:10.1007/JHEP08(2017)088, arXiv:1703.09252.

-
- [56] G. Buchalla et al., “Higgs boson pair production in non-linear effective field theory with full m_t -dependence at NLO QCD”, *JHEP* **09** (2018) 057, doi:10.1007/JHEP09(2018)057, arXiv:1806.05162.
- [57] J. Alwall et al., “The automated computation of tree-level and next-to-leading order differential cross sections, and their matching to parton shower simulations”, *JHEP* **07** (2014) 079, doi:10.1007/JHEP07(2014)079, arXiv:1405.0301.
- [58] J. Alwall et al., “Comparative study of various algorithms for the merging of parton showers and matrix elements in hadronic collisions”, *Eur. Phys. J. C* **53** (2008) 473, doi:10.1140/epjc/s10052-007-0490-5, arXiv:0706.2569.
- [59] R. Frederix and S. Frixione, “Merging meets matching in MC@NLO”, *JHEP* **12** (2012) 061, doi:10.1007/JHEP12(2012)061, arXiv:1209.6215.
- [60] CMS Collaboration, “Particle-flow reconstruction and global event description with the CMS detector”, *JINST* **12** (2017) P10003, doi:10.1088/1748-0221/12/10/P10003, arXiv:1706.04965.
- [61] M. Cacciari, G. P. Salam, and G. Soyez, “The anti- k_T jet clustering algorithm”, *JHEP* **04** (2008) 063, doi:10.1088/1126-6708/2008/04/063, arXiv:0802.1189.
- [62] M. Cacciari, G. P. Salam, and G. Soyez, “Fastjet user manual”, *Eur. Phys. J. C* **72** (2012) 1896, doi:10.1140/epjc/s10052-012-1896-2, arXiv:1111.6097.
- [63] CMS Collaboration, “Electron and photon reconstruction and identification with the CMS experiment at the CERN LHC”, 12, 2020. arXiv:2012.06888.
- [64] CMS Collaboration, “Performance of electron reconstruction and selection with the CMS detector in proton-proton collisions at $\sqrt{s} = 8$ TeV”, *JINST* **10** (2015) P06005, doi:10.1088/1748-0221/10/06/P06005, arXiv:1502.02701.
- [65] CMS Collaboration, “Performance of the CMS muon detector and muon reconstruction with proton-proton collisions at $\sqrt{s} = 13$ TeV”, *JINST* **13** (2018) P06015, doi:10.1088/1748-0221/13/06/P06015, arXiv:1804.04528.
- [66] M. Cacciari, G. P. Salam, and G. Soyez, “The catchment area of jets”, *JHEP* **04** (2008) 005, doi:10.1088/1126-6708/2008/04/005, arXiv:0802.1188.
- [67] CMS Collaboration, “Performance of reconstruction and identification of τ leptons decaying to hadrons and ν_τ in pp collisions at $\sqrt{s} = 13$ TeV”, *JINST* **13** (2018) P10005, doi:10.1088/1748-0221/13/10/P10005, arXiv:1809.02816.
- [68] CMS Collaboration, “Performance of the DeepTau algorithm for the discrimination of taus against jets, electrons, and muons”, CMS Detector Performance Summary CMS-DP-2019-033, 2019.
- [69] CMS Collaboration, “Jet algorithms performance in 13 TeV data”, CMS Physics Analysis Summary CMS-PAS-JME-16-003, 2016.
- [70] CMS Collaboration, “Identification of heavy-flavour jets with the CMS detector in pp collisions at 13 TeV”, *JINST* **13** (2018) P05011, doi:10.1088/1748-0221/13/05/P05011, arXiv:1712.07158.

- [71] M. Cacciari and G. P. Salam, “Pileup subtraction using jet areas”, *Phys. Lett. B* **659** (2008) 119, doi:10.1016/j.physletb.2007.09.077, arXiv:0707.1378.
- [72] CMS Collaboration, “Jet energy scale and resolution in the CMS experiment in pp collisions at 8 TeV”, *JINST* **12** (2017) P02014, doi:10.1088/1748-0221/12/02/P02014, arXiv:1607.03663.
- [73] CMS Collaboration, “Performance of missing transverse momentum reconstruction in proton-proton collisions at $\sqrt{s} = 13$ TeV using the CMS detector”, *JINST* **14** (2019) P07004, doi:10.1088/1748-0221/14/07/P07004, arXiv:1903.06078.
- [74] K. Ellis, I. Hinchliffe, Soldate, and J. van der Bij, “Higgs decay to $\tau^+\tau^-$: A possible signature of intermediate mass Higgs bosons at high energy hadron colliders”, *Nucl. Phys. B* **297** (1988) 221, doi:10.1016/0550-3213(88)90019-3.
- [75] H. Voss, A. Höcker, J. Stelzer, and F. Tegenfeldt, “TMVA, the toolkit for multivariate data analysis with ROOT”, in *XIth International Workshop on Advanced Computing and Analysis Techniques in Physics Research (ACAT)*, p. 40. 2007. arXiv:physics/0703039. [PoS(ACAT)040]. doi:10.22323/1.050.0040.
- [76] CMS Collaboration, “An embedding technique to determine $\tau\tau$ backgrounds in proton-proton collision data”, *JINST* **14** (2019) P06032, doi:10.1088/1748-0221/14/06/P06032, arXiv:1903.01216.
- [77] CMS Collaboration, “Observation of the Higgs boson decay to a pair of τ leptons with the CMS detector”, *Phys. Lett. B* **779** (2018) 283, doi:10.1016/j.physletb.2018.02.004, arXiv:1708.00373.
- [78] J. S. Conway, “Nuisance parameters in likelihoods for multisource spectra”, in *Proceedings of PHYSTAT 2011 Workshop on Statistical Issues Related to Discovery Claims in Search Experiments and Unfolding*, H. Propser and L. Lyons, eds., p. 115. CERN, 2011.
- [79] CMS Collaboration, “Measurements of inclusive W and Z cross sections in pp collisions at $\sqrt{s} = 7$ TeV”, *JHEP* **01** (2011) 080, doi:10.1007/JHEP01(2011)080, arXiv:1012.2466.
- [80] CMS Collaboration, “Performance of CMS muon reconstruction in pp collision events at $\sqrt{s} = 7$ TeV”, *JINST* **7** (2012) P10002, doi:10.1088/1748-0221/7/10/P10002, arXiv:1206.4071.
- [81] CMS Collaboration, “Reconstruction and identification of τ lepton decays to hadrons and ν_τ at CMS”, *JINST* **11** (2016) P01019, doi:10.1088/1748-0221/11/01/P01019, arXiv:1510.07488.
- [82] D. de Florian et al., “Handbook of LHC Higgs cross sections: 4. Deciphering the nature of the Higgs sector”, CERN Report CERN-2017-002-M, 2016. doi:10.23731/CYRM-2017-002, arXiv:1610.07922.
- [83] R. J. Barlow and C. Beeston, “Fitting using finite Monte Carlo samples”, *Comput. Phys. Commun.* **77** (1993) 219, doi:10.1016/0010-4655(93)90005-w.
- [84] CMS Collaboration, “CMS luminosity measurements for the 2016 data-taking period”, CMS Physics Analysis Summary CMS-PAS-LUM-17-001, 2017.

- [85] CMS Collaboration, “CMS luminosity measurement for the 2017 data-taking period at $\sqrt{s} = 13$ TeV”, CMS Physics Analysis Summary CMS-PAS-LUM-17-004, 2017.
- [86] CMS Collaboration, “CMS luminosity measurement for the 2018 data-taking period at $\sqrt{s} = 13$ TeV”, CMS Physics Analysis Summary CMS-PAS-LUM-18-002, 2018.
- [87] T. Junk, “Confidence level computation for combining searches with small statistics”, *Nucl. Instrum. Meth. A* **434** (1999) 435, doi:10.1016/S0168-9002(99)00498-2, arXiv:hep-ex/9902006.
- [88] A. L. Read, “Presentation of search results: The CL_s technique”, *J. Phys. G* **28** (2002) 2693, doi:10.1088/0954-3899/28/10/313.
- [89] G. Cowan, K. Cranmer, E. Gross, and O. Vitells, “Asymptotic formulae for likelihood-based tests of new physics”, *Eur. Phys. J. C* **71** (2011) 1554, doi:10.1140/epjc/s10052-011-1554-0, arXiv:1007.1727. [Erratum: doi:10.1140/epjc/s10052-013-2501-z].
- [90] A. Denner et al., “Standard model Higgs-boson branching ratios with uncertainties”, *Eur. Phys. J. C* **71** (2011) 1753, doi:10.1140/epjc/s10052-011-1753-8, arXiv:1107.5909.
- [91] “HEPData record for this analysis”. <https://www.hepdata.net/record/104861>.
- [92] K. Hayasaka et al., “Search for lepton flavor violating τ decays into three leptons with 719 million produced $\tau^+\tau^-$ pairs”, *Phys. Lett. B* **687** (2010) 139, doi:10.1016/j.physletb.2010.03.037, arXiv:1001.3221.
- [93] Belle Collaboration, “New search for $\tau \rightarrow \mu\gamma$ and $\tau \rightarrow e\gamma$ decays at Belle”, *Phys. Lett. B* **666** (2008) 16, doi:10.1016/j.physletb.2008.06.056, arXiv:0705.0650.

A The CMS Collaboration

Yerevan Physics Institute, Yerevan, Armenia

A.M. Sirunyan[†], A. Tumasyan

Institut für Hochenergiephysik, Wien, Austria

W. Adam, J.W. Andrejkovic, T. Bergauer, S. Chatterjee, M. Dragicevic, A. Escalante Del Valle, R. Frühwirth¹, M. Jeitler¹, N. Krammer, L. Lechner, D. Liko, I. Mikulec, P. Paulitsch, F.M. Pitters, J. Schieck¹, R. Schöfbeck, M. Spanring, S. Templ, W. Waltenberger, C.-E. Wulz¹

Institute for Nuclear Problems, Minsk, Belarus

V. Chekhovsky, A. Litomin, V. Makarenko

Universiteit Antwerpen, Antwerpen, Belgium

M.R. Darwish², E.A. De Wolf, X. Janssen, T. Kello³, A. Lelek, H. Rejeb Sfar, P. Van Mechelen, S. Van Putte, N. Van Remortel

Vrije Universiteit Brussel, Brussel, Belgium

F. Blekman, E.S. Bols, J. D'Hondt, J. De Clercq, M. Delcourt, H. El Faham, S. Lowette, S. Moortgat, A. Morton, D. Müller, A.R. Sahasransu, S. Tavernier, W. Van Doninck, P. Van Mulders

Université Libre de Bruxelles, Bruxelles, Belgium

D. Beghin, B. Bilin, B. Clerboux, G. De Lentdecker, L. Favart, A. Grebenyuk, A.K. Kalsi, K. Lee, M. Mahdavihorrami, I. Makarenko, L. Moureaux, L. Pétré, A. Popov, N. Postiau, E. Starling, L. Thomas, M. Vanden Bemden, C. Vander Velde, P. Vanlaer, D. Vannerom, L. Wezenbeek

Ghent University, Ghent, Belgium

T. Cornelis, D. Dobur, J. Knolle, L. Lambrecht, G. Mestdach, M. Niedziela, C. Roskas, A. Samalan, K. Skovpen, T.T. Tran, M. Tytgat, W. Verbeke, B. Vermassen, M. Vit

Université Catholique de Louvain, Louvain-la-Neuve, Belgium

A. Bethani, G. Bruno, F. Bury, C. Caputo, P. David, C. Delaere, I.S. Donertas, A. Giammanco, K. Jaffel, V. Lemaître, K. Mondal, J. Prisciandaro, A. Taliércio, M. Teklishyn, P. Vischia, S. Wertz, S. Wuyckens

Centro Brasileiro de Pesquisas Físicas, Rio de Janeiro, Brazil

G.A. Alves, C. Hensel, A. Moraes

Universidade do Estado do Rio de Janeiro, Rio de Janeiro, Brazil

W.L. Aldá Júnior, M. Alves Gallo Pereira, M. Barroso Ferreira Filho, H. BRANDAO MALBOUISSON, W. Carvalho, J. Chinellato⁴, E.M. Da Costa, G.G. Da Silveira⁵, D. De Jesus Damiao, S. Fonseca De Souza, D. Matos Figueiredo, C. Mora Herrera, K. Mota Amarilo, L. Mundim, H. Nogima, P. Rebello Teles, A. Santoro, S.M. Silva Do Amaral, A. Sznajder, M. Thiel, F. Torres Da Silva De Araujo, A. Vilela Pereira

Universidade Estadual Paulista ^a, Universidade Federal do ABC ^b, São Paulo, Brazil

C.A. Bernardes^{a,a}, L. Calligaris^a, T.R. Fernandez Perez Tomei^a, E.M. Gregores^{a,b}, D.S. Lemos^a, P.G. Mercadante^{a,b}, S.F. Novaes^a, Sandra S. Padula^a

Institute for Nuclear Research and Nuclear Energy, Bulgarian Academy of Sciences, Sofia, Bulgaria

A. Aleksandrov, G. Antchev, R. Hadjiiska, P. Iaydjiev, M. Misheva, M. Rodozov, M. Shopova, G. Sultanov

University of Sofia, Sofia, Bulgaria

A. Dimitrov, T. Ivanov, L. Litov, B. Pavlov, P. Petkov, A. Petrov

Beihang University, Beijing, China

T. Cheng, W. Fang³, Q. Guo, T. Javaid⁶, M. Mittal, H. Wang, L. Yuan

Department of Physics, Tsinghua University, Beijing, China

M. Ahmad, G. Bauer, C. Dozen⁷, Z. Hu, J. Martins⁸, Y. Wang, K. Yi^{9,10}

Institute of High Energy Physics, Beijing, China

E. Chapon, G.M. Chen⁶, H.S. Chen⁶, M. Chen, F. Iemmi, A. Kapoor, D. Leggat, H. Liao, Z.-A. LIU⁶, V. Milosevic, F. Monti, R. Sharma, J. Tao, J. Thomas-wilsker, J. Wang, H. Zhang, S. Zhang⁶, J. Zhao

State Key Laboratory of Nuclear Physics and Technology, Peking University, Beijing, China

A. Agapitos, Y. Ban, C. Chen, Q. Huang, A. Levin, Q. Li, X. Lyu, Y. Mao, S.J. Qian, D. Wang, Q. Wang, J. Xiao

Sun Yat-Sen University, Guangzhou, China

M. Lu, Z. You

Institute of Modern Physics and Key Laboratory of Nuclear Physics and Ion-beam Application (MOE) - Fudan University, Shanghai, China

X. Gao³, H. Okawa

Zhejiang University, Hangzhou, China

Z. Lin, M. Xiao

Universidad de Los Andes, Bogota, Colombia

C. Avila, A. Cabrera, C. Florez, J. Fraga, A. Sarkar, M.A. Segura Delgado

Universidad de Antioquia, Medellin, Colombia

J. Mejia Guisao, F. Ramirez, J.D. Ruiz Alvarez, C.A. Salazar González

University of Split, Faculty of Electrical Engineering, Mechanical Engineering and Naval Architecture, Split, Croatia

D. Giljanovic, N. Godinovic, D. Lelas, I. Puljak

University of Split, Faculty of Science, Split, Croatia

Z. Antunovic, M. Kovac, T. Sculac

Institute Rudjer Boskovic, Zagreb, Croatia

V. Brigljevic, D. Ferencek, D. Majumder, M. Roguljic, A. Starodumov¹¹, T. Susa

University of Cyprus, Nicosia, Cyprus

A. Attikis, E. Erodotou, A. Ioannou, G. Kole, M. Kolosova, S. Konstantinou, J. Mousa, C. Nicolaou, F. Ptochos, P.A. Razis, H. Rykaczewski, H. Saka

Charles University, Prague, Czech Republic

M. Finger¹², M. Finger Jr.¹², A. Kveton

Escuela Politecnica Nacional, Quito, Ecuador

E. Ayala

Universidad San Francisco de Quito, Quito, Ecuador

E. Carrera Jarrin

Academy of Scientific Research and Technology of the Arab Republic of Egypt, Egyptian Network of High Energy Physics, Cairo, Egypt

H. Abdalla¹³, A. Ellithi Kamel¹³

Center for High Energy Physics (CHEP-FU), Fayoum University, El-Fayoum, Egypt

A. Lotfy, M.A. Mahmoud

National Institute of Chemical Physics and Biophysics, Tallinn, Estonia

S. Bhowmik, A. Carvalho Antunes De Oliveira, R.K. Dewanjee, K. Ehataht, M. Kadastik, C. Nielsen, J. Pata, M. Raidal, L. Tani, C. Veelken

Department of Physics, University of Helsinki, Helsinki, Finland

P. Eerola, L. Forthomme, H. Kirschenmann, K. Osterberg, M. Voutilainen

Helsinki Institute of Physics, Helsinki, Finland

S. Bharthuar, E. Brücken, F. Garcia, J. Havukainen, M.S. Kim, R. Kinnunen, T. Lampén, K. Lassila-Perini, S. Lehti, T. Lindén, M. Lotti, L. Martikainen, J. Ott, H. Siikonen, E. Tuominen, J. Tuominiemi

Lappeenranta University of Technology, Lappeenranta, Finland

P. Luukka, H. Petrow, T. Tuuva

IRFU, CEA, Université Paris-Saclay, Gif-sur-Yvette, France

C. Amendola, M. Besancon, F. Couderc, M. Dejardin, D. Denegri, J.L. Faure, F. Ferri, S. Ganjour, A. Givernaud, P. Gras, G. Hamel de Monchenault, P. Jarry, B. Lenzi, E. Locci, J. Malcles, J. Rander, A. Rosowsky, M.Ö. Sahin, A. Savoy-Navarro¹⁴, M. Titov, G.B. Yu

Laboratoire Leprince-Ringuet, CNRS/IN2P3, Ecole Polytechnique, Institut Polytechnique de Paris, Palaiseau, France

S. Ahuja, F. Beaudette, M. Bonanomi, A. Buchot Perraguin, P. Busson, A. Cappati, C. Charlot, O. Davignon, B. Diab, G. Falmagne, S. Ghosh, R. Granier de Cassagnac, A. Hakimi, I. Kucher, M. Nguyen, C. Ochando, P. Paganini, J. Rembser, R. Salerno, J.B. Sauvan, Y. Sirois, A. Zabi, A. Zghiche

Université de Strasbourg, CNRS, IPHC UMR 7178, Strasbourg, France

J.-L. Agram¹⁵, J. Andrea, D. Apparau, D. Bloch, G. Bourgatte, J.-M. Brom, E.C. Chabert, C. Collard, D. Darej, J.-C. Fontaine¹⁵, U. Goerlach, C. Grimault, A.-C. Le Bihan, E. Nibigira, P. Van Hove

Institut de Physique des 2 Infinis de Lyon (IP2I), Villeurbanne, France

E. Asilar, S. Beauceron, C. Bernet, G. Boudoul, C. Camen, A. Carle, N. Chanon, D. Contardo, P. Depasse, H. El Mamouni, J. Fay, S. Gascon, M. Gouzevitch, B. Ille, Sa. Jain, I.B. Laktineh, H. Lattaud, A. Lesauvage, M. Lethuillier, L. Mirabito, S. Perries, K. Shchablo, V. Sordini, L. Torterotot, G. Touquet, M. Vander Donckt, S. Viret

Georgian Technical University, Tbilisi, Georgia

A. Khvedelidze¹², I. Lomidze, Z. Tsamalaidze¹²

RWTH Aachen University, I. Physikalisches Institut, Aachen, Germany

L. Feld, K. Klein, M. Lipinski, D. Meuser, A. Pauls, M.P. Rauch, N. Röwert, J. Schulz, M. Teroerde

RWTH Aachen University, III. Physikalisches Institut A, Aachen, Germany

D. Eliseev, M. Erdmann, P. Fackeldey, B. Fischer, S. Ghosh, T. Hebbeker, K. Hoepfner, F. Ivone, H. Keller, L. Mastrolorenzo, M. Merschmeyer, A. Meyer, G. Mocellin, S. Mondal, S. Mukherjee,

D. Noll, A. Novak, T. Pook, A. Pozdnyakov, Y. Rath, H. Reithler, J. Roemer, A. Schmidt, S.C. Schuler, A. Sharma, S. Wiedenbeck, S. Zaleski

RWTH Aachen University, III. Physikalisches Institut B, Aachen, Germany

C. Dziwok, G. Flügge, W. Haj Ahmad¹⁶, O. Hlushchenko, T. Kress, A. Nowack, C. Pistone, O. Pooth, D. Roy, H. Sert, A. Stahl¹⁷, T. Ziemons

Deutsches Elektronen-Synchrotron, Hamburg, Germany

H. Aarup Petersen, M. Aldaya Martin, P. Asmuss, I. Babounikau, S. Baxter, O. Behnke, A. Bermúdez Martínez, S. Bhattacharya, A.A. Bin Anuar, K. Borras¹⁸, V. Botta, D. Brunner, A. Campbell, A. Cardini, C. Cheng, F. Colombina, S. Consuegra Rodríguez, G. Correia Silva, V. Danilov, L. Didukh, G. Eckerlin, D. Eckstein, L.I. Estevez Banos, O. Filatov, E. Gallo¹⁹, A. Geiser, A. Giraldi, A. Grohsjean, M. Guthoff, A. Jafari²⁰, N.Z. Jomhari, H. Jung, A. Kasem¹⁸, M. Kasemann, H. Kaveh, C. Kleinwort, D. Krücker, W. Lange, J. Lidrych, K. Lipka, W. Lohmann²¹, R. Mankel, I.-A. Melzer-Pellmann, J. Metwally, A.B. Meyer, M. Meyer, J. Mnich, A. Mussgiller, Y. Otariid, D. Pérez Adán, D. Pitzl, A. Raspereza, B. Ribeiro Lopes, J. Rübenach, A. Saggio, A. Saibel, M. Savitskyi, M. Scham, V. Scheurer, C. Schwanenberger¹⁹, A. Singh, R.E. Sosa Ricardo, D. Stafford, N. Tonon, O. Turkot, M. Van De Klundert, R. Walsh, D. Walter, Y. Wen, K. Wichmann, L. Wiens, C. Wissing, S. Wuchterl

University of Hamburg, Hamburg, Germany

R. Aggleton, S. Bein, L. Benato, A. Benecke, P. Connor, K. De Leo, M. Eich, F. Feindt, A. Fröhlich, C. Garbers, E. Garutti, P. Gunnellini, J. Haller, A. Hinzmann, G. Kasieczka, R. Klanner, R. Kogler, T. Kramer, V. Kutzner, J. Lange, T. Lange, A. Lobanov, A. Malara, A. Nigamova, K.J. Pena Rodriguez, O. Rieger, P. Schleper, M. Schröder, J. Schwandt, D. Schwarz, J. Sonneveld, H. Stadie, G. Steinbrück, A. Tews, B. Vormwald, I. Zoi

Karlsruher Institut fuer Technologie, Karlsruhe, Germany

J. Bechtel, T. Berger, E. Butz, R. Caspart, T. Chwalek, W. De Boer[†], A. Dierlamm, A. Droll, K. El Morabit, N. Faltermann, M. Giffels, J.o. Gosewisch, A. Gottmann, F. Hartmann¹⁷, C. Heidecker, U. Husemann, I. Katkov²², P. Keicher, R. Koppenhöfer, S. Maier, M. Metzler, S. Mitra, Th. Müller, M. Neukum, A. Nürnberg, G. Quast, K. Rabbertz, J. Rauser, D. Savoie, M. Schnepf, D. Seith, I. Shvetsov, H.J. Simonis, R. Ulrich, J. Van Der Linden, R.F. Von Cube, M. Wassmer, M. Weber, S. Wieland, R. Wolf, S. Wozniewski, S. Wunsch

Institute of Nuclear and Particle Physics (INPP), NCSR Demokritos, Aghia Paraskevi, Greece

G. Anagnostou, P. Asenov, G. Daskalakis, T. Gerasis, A. Kyriakis, D. Loukas, A. Stakia

National and Kapodistrian University of Athens, Athens, Greece

M. Diamantopoulou, D. Karasavvas, G. Karathanasis, P. Kontaxakis, C.K. Koraka, A. Manousakis-katsikakis, A. Panagiotou, I. Papavergou, N. Saoulidou, K. Theofilatos, E. Tziaferi, K. Vellidis, E. Vourliotis

National Technical University of Athens, Athens, Greece

G. Bakas, K. Kousouris, I. Papakrivopoulos, G. Tsipolitis, A. Zacharopoulou

University of Ioánnina, Ioánnina, Greece

I. Evangelou, C. Foudas, P. Gianneios, P. Katsoulis, P. Kokkas, N. Manthos, I. Papadopoulos, J. Strologas

MTA-ELTE Lendület CMS Particle and Nuclear Physics Group, Eötvös Loránd University,

Budapest, Hungary

M. Csanad, K. Farkas, M.M.A. Gadallah²³, S. Lökös²⁴, P. Major, K. Mandal, A. Mehta, G. Pasztor, A.J. Rádl, O. Surányi, G.I. Veres

Wigner Research Centre for Physics, Budapest, Hungary

M. Bartók²⁵, G. Bencze, C. Hajdu, D. Horvath²⁶, F. Sikler, V. Veszpremi, G. Vesztergombi[†]

Institute of Nuclear Research ATOMKI, Debrecen, Hungary

S. Czellar, J. Karancsi²⁵, J. Molnar, Z. Szillasi, D. Teyssier

Institute of Physics, University of Debrecen, Debrecen, Hungary

P. Raics, Z.L. Trocsanyi²⁷, B. Ujvari

Eszterhazy Karoly University, Karoly Robert Campus, Gyongyos, Hungary

T. Csorgo²⁸, F. Nemes²⁸, T. Novak

Indian Institute of Science (IISc), Bangalore, India

J.R. Komaragiri, D. Kumar, L. Panwar, P.C. Tiwari

National Institute of Science Education and Research, HBNI, Bhubaneswar, India

S. Bahinipati²⁹, D. Dash, C. Kar, P. Mal, T. Mishra, V.K. Muraleedharan Nair Bindhu³⁰, A. Nayak³⁰, P. Saha, N. Sur, S.K. Swain, D. Vats³⁰

Panjab University, Chandigarh, India

S. Bansal, S.B. Beri, V. Bhatnagar, G. Chaudhary, S. Chauhan, N. Dhingra³¹, R. Gupta, A. Kaur, M. Kaur, S. Kaur, P. Kumari, M. Meena, K. Sandeep, J.B. Singh, A.K. Viridi

University of Delhi, Delhi, India

A. Ahmed, A. Bhardwaj, B.C. Choudhary, M. Gola, S. Keshri, A. Kumar, M. Naimuddin, P. Priyanka, K. Ranjan, A. Shah

Saha Institute of Nuclear Physics, HBNI, Kolkata, India

M. Bharti³², R. Bhattacharya, S. Bhattacharya, D. Bhowmik, S. Dutta, S. Dutta, B. Gomber³³, M. Maity³⁴, S. Nandan, P. Palit, P.K. Rout, G. Saha, B. Sahu, S. Sarkar, M. Sharan, B. Singh³², S. Thakur³²

Indian Institute of Technology Madras, Madras, India

P.K. Behera, S.C. Behera, P. Kalbhor, A. Muhammad, R. Pradhan, P.R. Pujahari, A. Sharma, A.K. Sikdar

Bhabha Atomic Research Centre, Mumbai, India

D. Dutta, V. Jha, V. Kumar, D.K. Mishra, K. Naskar³⁵, P.K. Netrakanti, L.M. Pant, P. Shukla

Tata Institute of Fundamental Research-A, Mumbai, India

T. Aziz, S. Dugad, M. Kumar, U. Sarkar

Tata Institute of Fundamental Research-B, Mumbai, India

S. Banerjee, R. Chudasama, M. Guchait, S. Karmakar, S. Kumar, G. Majumder, K. Mazumdar, S. Mukherjee

Indian Institute of Science Education and Research (IISER), Pune, India

K. Alpana, S. Dube, B. Kansal, S. Pandey, A. Rane, A. Rastogi, S. Sharma

Department of Physics, Isfahan University of Technology, Isfahan, Iran

H. Bakhshiansohi³⁶, M. Zeinali³⁷

Institute for Research in Fundamental Sciences (IPM), Tehran, IranS. Chenarani³⁸, S.M. Etesami, M. Khakzad, M. Mohammadi Najafabadi**University College Dublin, Dublin, Ireland**

M. Grunewald

INFN Sezione di Bari ^a, Università di Bari ^b, Politecnico di Bari ^c, Bari, ItalyM. Abbrescia^{a,b}, R. Aly^{a,b,39}, C. Aruta^{a,b}, A. Colaleo^a, D. Creanza^{a,c}, N. De Filippis^{a,c}, M. De Palma^{a,b}, A. Di Florio^{a,b}, A. Di Pilato^{a,b}, W. Elmetenawee^{a,b}, L. Fiore^a, A. Gelmi^{a,b}, M. Gul^a, G. Iaselli^{a,c}, M. Ince^{a,b}, S. Lezki^{a,b}, G. Maggi^{a,c}, M. Maggi^a, I. Margjeka^{a,b}, V. Mastrapasqua^{a,b}, J.A. Merlin^a, S. My^{a,b}, S. Nuzzo^{a,b}, A. Pellecchia^{a,b}, A. Pompili^{a,b}, G. Pugliese^{a,c}, A. Ranieri^a, G. Selvaggi^{a,b}, L. Silvestris^a, F.M. Simone^{a,b}, R. Venditti^a, P. Verwilligen^a**INFN Sezione di Bologna ^a, Università di Bologna ^b, Bologna, Italy**G. Abbiendi^a, C. Battilana^{a,b}, D. Bonacorsi^{a,b}, L. Borghonovi^a, L. Brigliadori^a, R. Campanini^{a,b}, P. Capiluppi^{a,b}, A. Castro^{a,b}, F.R. Cavallo^a, M. Cuffiani^{a,b}, G.M. Dallavalle^a, T. Diotallevi^{a,b}, F. Fabbri^a, A. Fanfani^{a,b}, P. Giacomelli^a, L. Giommi^{a,b}, C. Grandi^a, L. Guiducci^{a,b}, S. Lo Meo^{a,40}, L. Lunerti^{a,b}, S. Marcellini^a, G. Masetti^a, F.L. Navarra^{a,b}, A. Perrotta^a, F. Primavera^{a,b}, A.M. Rossi^{a,b}, T. Rovelli^{a,b}, G.P. Siroli^{a,b}**INFN Sezione di Catania ^a, Università di Catania ^b, Catania, Italy**S. Albergo^{a,b,41}, S. Costa^{a,b,41}, A. Di Mattia^a, R. Potenza^{a,b}, A. Tricomi^{a,b,41}, C. Tuve^{a,b}**INFN Sezione di Firenze ^a, Università di Firenze ^b, Firenze, Italy**G. Barbagli^a, A. Cassese^a, R. Ceccarelli^{a,b}, V. Ciulli^{a,b}, C. Civinini^a, R. D'Alessandro^{a,b}, E. Focardi^{a,b}, G. Latino^{a,b}, P. Lenzi^{a,b}, M. Lizzo^{a,b}, M. Meschini^a, S. Paoletti^a, R. Seidita^{a,b}, G. Sguazzoni^a, L. Viliani^a**INFN Laboratori Nazionali di Frascati, Frascati, Italy**

L. Benussi, S. Bianco, D. Piccolo

INFN Sezione di Genova ^a, Università di Genova ^b, Genova, ItalyM. Bozzo^{a,b}, F. Ferro^a, R. Mulargia^{a,b}, E. Robutti^a, S. Tosi^{a,b}**INFN Sezione di Milano-Bicocca ^a, Università di Milano-Bicocca ^b, Milano, Italy**A. Benaglia^a, F. Brivio^{a,b}, F. Cetorelli^{a,b}, V. Ciriolo^{a,b,17}, F. De Guio^{a,b}, M.E. Dinardo^{a,b}, P. Dini^a, S. Gennai^a, A. Ghezzi^{a,b}, P. Govoni^{a,b}, L. Guzzi^{a,b}, M. Malberti^a, S. Malvezzi^a, A. Massironi^a, D. Menasce^a, L. Moroni^a, M. Paganoni^{a,b}, D. Pedrini^a, S. Ragazzi^{a,b}, N. Redaelli^a, T. Tabarelli de Fatis^{a,b}, D. Valsecchi^{a,b,17}, D. Zuolo^{a,b}**INFN Sezione di Napoli ^a, Università di Napoli 'Federico II' ^b, Napoli, Italy, Università della Basilicata ^c, Potenza, Italy, Università G. Marconi ^d, Roma, Italy**S. Buontempo^a, F. Carnevali^{a,b}, N. Cavallo^{a,c}, A. De Iorio^{a,b}, F. Fabozzi^{a,c}, A.O.M. Iorio^{a,b}, L. Lista^{a,b}, S. Meola^{a,d,17}, P. Paolucci^{a,17}, B. Rossi^a, C. Sciacca^{a,b}**INFN Sezione di Padova ^a, Università di Padova ^b, Padova, Italy, Università di Trento ^c, Trento, Italy**P. Azzi^a, N. Bacchetta^a, D. Bisello^{a,b}, P. Bortignon^a, A. Bragagnolo^{a,b}, R. Carlin^{a,b}, P. Checchia^a, T. Dorigo^a, U. Dosselli^a, F. Gasparini^{a,b}, U. Gasparini^{a,b}, S.Y. Hoh^{a,b}, L. Layer^{a,42}, M. Margoni^{a,b}, A.T. Meneguzzo^{a,b}, J. Pazzini^{a,b}, M. Presilla^{a,b}, P. Ronchese^{a,b}, R. Rossin^{a,b}, F. Simonetto^{a,b}, G. Strong^a, M. Tosi^{a,b}, H. YARAR^{a,b}, M. Zanetti^{a,b}, P. Zotto^{a,b}, A. Zucchetta^{a,b}, G. Zumerle^{a,b}

INFN Sezione di Pavia ^a, Università di Pavia ^b, Pavia, Italy

C. Aime^{a,b}, A. Braghieri^a, S. Calzaferri^{a,b}, D. Fiorina^{a,b}, P. Montagna^{a,b}, S.P. Ratti^{a,b}, V. Re^a, C. Riccardi^{a,b}, P. Salvini^a, I. Vai^a, P. Vitulo^{a,b}

INFN Sezione di Perugia ^a, Università di Perugia ^b, Perugia, Italy

G.M. Bilei^a, D. Ciangottini^{a,b}, L. Fanò^{a,b}, P. Lariccia^{a,b}, M. Magherini^b, G. Mantovani^{a,b}, V. Mariani^{a,b}, M. Menichelli^a, F. Moscatelli^a, A. Piccinelli^{a,b}, A. Rossi^{a,b}, A. Santocchia^{a,b}, D. Spiga^a, T. Tedeschi^{a,b}

INFN Sezione di Pisa ^a, Università di Pisa ^b, Scuola Normale Superiore di Pisa ^c, Pisa Italy, Università di Siena ^d, Siena, Italy

P. Azzurri^a, G. Bagliesi^a, V. Bertacchi^{a,c}, L. Bianchini^a, T. Boccali^a, E. Bossini^{a,b}, R. Castaldi^a, M.A. Ciocci^{a,b}, R. Dell'Orso^a, M.R. Di Domenico^{a,d}, S. Donato^a, A. Giassi^a, M.T. Grippo^a, F. Ligabue^{a,c}, E. Manca^{a,c}, G. Mandorli^{a,c}, A. Messineo^{a,b}, F. Palla^a, S. Parolia^{a,b}, G. Ramirez-Sanchez^{a,c}, A. Rizzi^{a,b}, G. Rolandi^{a,c}, S. Roy Chowdhury^{a,c}, A. Scribano^a, N. Shafiei^{a,b}, P. Spagnolo^a, R. Tenchini^a, G. Tonelli^{a,b}, N. Turini^{a,d}, A. Venturi^a, P.G. Verdini^a

INFN Sezione di Roma ^a, Sapienza Università di Roma ^b, Rome, Italy

M. Campana^{a,b}, F. Cavallari^a, M. Cipriani^{a,b}, D. Del Re^{a,b}, E. Di Marco^a, M. Diemoz^a, E. Longo^{a,b}, P. Meridiani^a, G. Organtini^{a,b}, F. Pandolfi^a, R. Paramatti^{a,b}, C. Quaranta^{a,b}, S. Rahatlou^{a,b}, C. Rovelli^a, F. Santanastasio^{a,b}, L. Soffia^a, R. Tramontano^{a,b}

INFN Sezione di Torino ^a, Università di Torino ^b, Torino, Italy, Università del Piemonte Orientale ^c, Novara, Italy

N. Amapane^{a,b}, R. Arcidiacono^{a,c}, S. Argiro^{a,b}, M. Arneodo^{a,c}, N. Bartosik^a, R. Bellan^{a,b}, A. Bellora^{a,b}, J. Berenguer Antequera^{a,b}, C. Biino^a, N. Cartiglia^a, S. Cometti^a, M. Costa^{a,b}, R. Covarelli^{a,b}, N. Demaria^a, B. Kiani^{a,b}, F. Legger^a, C. Mariotti^a, S. Maselli^a, E. Migliore^{a,b}, E. Monteil^{a,b}, M. Monteno^a, M.M. Obertino^{a,b}, G. Ortona^a, L. Pacher^{a,b}, N. Pastrone^a, M. Pelliccioni^a, G.L. Pinna Angioni^{a,b}, M. Ruspa^{a,c}, R. Salvatico^{a,b}, K. Shchelina^{a,b}, F. Siviero^{a,b}, V. Sola^a, A. Solano^{a,b}, D. Soldi^{a,b}, A. Staiano^a, M. Tornago^{a,b}, D. Trocino^{a,b}, A. Vagnerini

INFN Sezione di Trieste ^a, Università di Trieste ^b, Trieste, Italy

S. Belforte^a, V. Candelise^{a,b}, M. Casarsa^a, F. Cossutti^a, A. Da Rold^{a,b}, G. Della Ricca^{a,b}, G. Sorrentino^{a,b}, F. Vazzoler^{a,b}

Kyungpook National University, Daegu, Korea

S. Dogra, C. Huh, B. Kim, D.H. Kim, G.N. Kim, J. Kim, J. Lee, S.W. Lee, C.S. Moon, Y.D. Oh, S.I. Pak, B.C. Radburn-Smith, S. Sekmen, Y.C. Yang

Chonnam National University, Institute for Universe and Elementary Particles, Kwangju, Korea

H. Kim, D.H. Moon

Hanyang University, Seoul, Korea

B. Francois, T.J. Kim, J. Park

Korea University, Seoul, Korea

S. Cho, S. Choi, Y. Go, B. Hong, K. Lee, K.S. Lee, J. Lim, J. Park, S.K. Park, J. Yoo

Kyung Hee University, Department of Physics, Seoul, Republic of Korea

J. Goh, A. Gurtu

Sejong University, Seoul, Korea

H.S. Kim, Y. Kim

Seoul National University, Seoul, Korea

J. Almond, J.H. Bhyun, J. Choi, S. Jeon, J. Kim, J.S. Kim, S. Ko, H. Kwon, H. Lee, S. Lee, B.H. Oh, M. Oh, S.B. Oh, H. Seo, U.K. Yang, I. Yoon

University of Seoul, Seoul, Korea

W. Jang, D. Jeon, D.Y. Kang, Y. Kang, J.H. Kim, S. Kim, B. Ko, J.S.H. Lee, Y. Lee, I.C. Park, Y. Roh, M.S. Ryu, D. Song, I.J. Watson, S. Yang

Yonsei University, Department of Physics, Seoul, Korea

S. Ha, H.D. Yoo

Sungkyunkwan University, Suwon, Korea

Y. Jeong, H. Lee, Y. Lee, I. Yu

College of Engineering and Technology, American University of the Middle East (AUM), Egaila, Kuwait

T. Beyrouthy, Y. Maghrbi

Riga Technical University, Riga, Latvia

V. Veckalns⁴³

Vilnius University, Vilnius, Lithuania

M. Ambrozas, A. Juodagalvis, A. Rinkevicius, G. Tamulaitis, A. Vaitkevicius

National Centre for Particle Physics, Universiti Malaya, Kuala Lumpur, Malaysia

N. Bin Norjoharuddeen, W.A.T. Wan Abdullah, M.N. Yusli, Z. Zolkapli

Universidad de Sonora (UNISON), Hermosillo, Mexico

J.F. Benitez, A. Castaneda Hernandez, M. León Coello, J.A. Murillo Quijada, A. Sehrawat, L. Valencia Palomo

Centro de Investigacion y de Estudios Avanzados del IPN, Mexico City, Mexico

G. Ayala, H. Castilla-Valdez, I. Heredia-De La Cruz⁴⁴, R. Lopez-Fernandez, C.A. Mondragon Herrera, D.A. Perez Navarro, A. Sanchez-Hernandez

Universidad Iberoamericana, Mexico City, Mexico

S. Carrillo Moreno, C. Oropeza Barrera, M. Ramirez-Garcia, F. Vazquez Valencia

Benemerita Universidad Autonoma de Puebla, Puebla, Mexico

I. Pedraza, H.A. Salazar Ibarguen, C. Uribe Estrada

University of Montenegro, Podgorica, Montenegro

J. Mijuskovic⁴⁵, N. Raicevic

University of Auckland, Auckland, New Zealand

D. Krofcheck

University of Canterbury, Christchurch, New Zealand

S. Bheesette, P.H. Butler

National Centre for Physics, Quaid-I-Azam University, Islamabad, Pakistan

A. Ahmad, M.I. Asghar, A. Awais, M.I.M. Awan, H.R. Hoorani, W.A. Khan, M.A. Shah, M. Shoaib, M. Waqas

AGH University of Science and Technology Faculty of Computer Science, Electronics and Telecommunications, Krakow, Poland

V. Avati, L. Grzanka, M. Malawski

National Centre for Nuclear Research, Swierk, Poland

H. Bialkowska, M. Bluj, B. Boimska, M. Górski, M. Kazana, M. Szeleper, P. Zalewski

Institute of Experimental Physics, Faculty of Physics, University of Warsaw, Warsaw, Poland

K. Bunkowski, K. Doroba, A. Kalinowski, M. Konecki, J. Krolikowski, M. Walczak

Laboratório de Instrumentação e Física Experimental de Partículas, Lisboa, Portugal

M. Araujo, P. Bargassa, D. Bastos, A. Boletti, P. Faccioli, M. Gallinaro, J. Hollar, N. Leonardo, T. Niknejad, M. Pisano, J. Seixas, O. Toldaiev, J. Varela

Joint Institute for Nuclear Research, Dubna, Russia

S. Afanasiev, D. Budkouski, I. Golutvin, I. Gorbunov, V. Karjavine, V. Korenkov, A. Lanev, A. Malakhov, V. Matveev^{46,47}, V. Palichik, V. Perelygin, M. Savina, D. Seitova, V. Shalaev, S. Shmatov, S. Shulha, V. Smirnov, O. Teryaev, N. Voytishin, B.S. Yuldashev⁴⁸, A. Zarubin, I. Zhizhin

Petersburg Nuclear Physics Institute, Gatchina (St. Petersburg), Russia

G. Gavrillov, V. Golovtsov, Y. Ivanov, V. Kim⁴⁹, E. Kuznetsova⁵⁰, V. Murzin, V. Oreshkin, I. Smirnov, D. Sosnov, V. Sulimov, L. Uvarov, S. Volkov, A. Vorobyev

Institute for Nuclear Research, Moscow, Russia

Yu. Andreev, A. Dermenev, S. Gninenko, N. Golubev, A. Karneyeu, D. Kirpichnikov, M. Kirsanov, N. Krasnikov, A. Pashenkov, G. Pivovarov, D. Tlisov[†], A. Toropin

Institute for Theoretical and Experimental Physics named by A.I. Alikhanov of NRC 'Kurchatov Institute', Moscow, Russia

V. Epshteyn, V. Gavrillov, N. Lychkovskaya, A. Nikitenko⁵¹, V. Popov, A. Spiridonov, A. Steppenov, M. Toms, E. Vlasov, A. Zhokin

Moscow Institute of Physics and Technology, Moscow, Russia

T. Aushev

National Research Nuclear University 'Moscow Engineering Physics Institute' (MEPhI), Moscow, Russia

O. Bychkova, R. Chistov⁵², M. Danilov⁵³, P. Parygin, S. Polikarpov⁵²

P.N. Lebedev Physical Institute, Moscow, Russia

V. Andreev, M. Azarkin, I. Dremin, M. Kirakosyan, A. Terkulov

Skobeltsyn Institute of Nuclear Physics, Lomonosov Moscow State University, Moscow, Russia

A. Belyaev, E. Boos, V. Bunichev, M. Dubinin⁵⁴, L. Dudko, A. Ershov, A. Gribushin, V. Klyukhin, O. Kodolova, I. Lokhtin, S. Obraztsov, M. Perfilov, V. Savrin

Novosibirsk State University (NSU), Novosibirsk, Russia

V. Blinov⁵⁵, T. Dimova⁵⁵, L. Kardapoltsev⁵⁵, A. Kozyrev⁵⁵, I. Ovtin⁵⁵, Y. Skovpen⁵⁵

Institute for High Energy Physics of National Research Centre 'Kurchatov Institute', Protvino, Russia

I. Azhgirey, I. Bayshev, D. Elumakhov, V. Kachanov, D. Konstantinov, P. Mandrik, V. Petrov, R. Ryutin, S. Slabospitskii, A. Sobol, S. Troshin, N. Tyurin, A. Uzunian, A. Volkov

National Research Tomsk Polytechnic University, Tomsk, Russia

A. Babaev, V. Okhotnikov

Tomsk State University, Tomsk, Russia

V. Borchsh, V. Ivanchenko, E. Tcherniaev

University of Belgrade: Faculty of Physics and VINCA Institute of Nuclear Sciences, Belgrade, SerbiaP. Adzic⁵⁶, M. Dordevic, P. Milenovic, J. Milosevic**Centro de Investigaciones Energéticas Medioambientales y Tecnológicas (CIEMAT), Madrid, Spain**

M. Aguilar-Benitez, J. Alcaraz Maestre, A. Álvarez Fernández, I. Bachiller, M. Barrio Luna, Cristina F. Bedoya, C.A. Carrillo Montoya, M. Cepeda, M. Cerrada, N. Colino, B. De La Cruz, A. Delgado Peris, J.P. Fernández Ramos, J. Flix, M.C. Fouz, O. Gonzalez Lopez, S. Goy Lopez, J.M. Hernandez, M.I. Josa, J. León Holgado, D. Moran, Á. Navarro Tobar, A. Pérez-Calero Yzquierdo, J. Puerta Pelayo, I. Redondo, L. Romero, S. Sánchez Navas, L. Urda Gómez, C. Willmott

Universidad Autónoma de Madrid, Madrid, Spain

J.F. de Trocóniz, R. Reyes-Almanza

Universidad de Oviedo, Instituto Universitario de Ciencias y Tecnologías Espaciales de Asturias (ICTEA), Oviedo, Spain

B. Alvarez Gonzalez, J. Cuevas, C. Erice, J. Fernandez Menendez, S. Folgueras, I. Gonzalez Caballero, E. Palencia Cortezon, C. Ramón Álvarez, J. Ripoll Sau, V. Rodríguez Bouza, A. Trapote, N. Trevisani

Instituto de Física de Cantabria (IFCA), CSIC-Universidad de Cantabria, Santander, Spain

J.A. Brochero Cifuentes, I.J. Cabrillo, A. Calderon, J. Duarte Campderros, M. Fernandez, C. Fernandez Madrazo, P.J. Fernández Manteca, A. García Alonso, G. Gomez, C. Martinez Rivero, P. Martinez Ruiz del Arbol, F. Matorras, P. Matorras Cuevas, J. Piedra Gomez, C. Prieels, T. Rodrigo, A. Ruiz-Jimeno, L. Scodellaro, I. Vila, J.M. Vizán Garcia

University of Colombo, Colombo, Sri LankaMK Jayananda, B. Kailaspathy⁵⁷, D.U.J. Sonnadara, DDC Wickramarathna**University of Ruhuna, Department of Physics, Matara, Sri Lanka**

W.G.D. Dharmaratna, K. Liyanage, N. Perera, N. Wickramage

CERN, European Organization for Nuclear Research, Geneva, SwitzerlandT.K. Aarrestad, D. Abbaneo, J. Alimena, E. Auffray, G. Auzinger, J. Baechler, P. Baillon[†], D. Barney, J. Bendavid, M. Bianco, A. Bocchi, T. Camporesi, M. Capeans Garrido, G. Cerminara, S.S. Chhibra, L. Cristella, D. d'Enterria, A. Dabrowski, N. Daci, A. David, A. De Roeck, M.M. Defranchis, M. Deile, M. Dobson, M. Dünser, N. Dupont, A. Elliott-Peisert, N. Emriskova, F. Fallavollita⁵⁸, D. Fasanella, S. Fiorendi, A. Florent, G. Franzoni, W. Funk, S. Giani, D. Gigi, K. Gill, F. Glege, L. Gouskos, M. Haranko, J. Hegeman, Y. Iiyama, V. Innocente, T. James, P. Janot, J. Kaspar, J. Kieseler, M. Komm, N. Kratochwil, C. Lange, S. Laurila, P. Lecoq, K. Long, C. Lourenço, L. Malgeri, S. Mallios, M. Mannelli, A.C. Marini, F. Meijers, S. Mersi, E. Meschi, F. Moortgat, M. Mulders, S. Orfanelli, L. Orsini, F. Pantaleo, L. Pape, E. Perez, M. Peruzzi, A. Petrilli, G. Petrucciani, A. Pfeiffer, M. Pierini, D. Piparo, M. Pitt, H. Qu, T. Quast, D. Rabadý, A. Racz, G. Reales Gutiérrez, M. Rieger, M. Rovere, H. Sakulin, J. Salfeld-Nebgen, S. Scarfi, C. Schäfer, C. Schwick, M. Selvaggi, A. Sharma, P. Silva, W. Snoeys, P. Sphicas⁵⁹, S. Summers, V.R. Tavolaro, D. Treille, A. Tsiros, G.P. Van Onsem, M. Verzetti, J. Wanczyk⁶⁰, K.A. Wozniak, W.D. Zeuner

Paul Scherrer Institut, Villigen, Switzerland

L. Caminada⁶¹, A. Ebrahimi, W. Erdmann, R. Horisberger, Q. Ingram, H.C. Kaestli, D. Kotlinski, U. Langenegger, M. Missiroli, T. Rohe

ETH Zurich - Institute for Particle Physics and Astrophysics (IPA), Zurich, Switzerland

K. Androsov⁶⁰, M. Backhaus, P. Berger, A. Calandri, N. Chernyavskaya, A. De Cosa, G. Dissertori, M. Dittmar, M. Donegà, C. Dorfer, F. Eble, T.A. Gómez Espinosa, C. Grab, D. Hits, W. Lustermann, A.-M. Lyon, R.A. Manzoni, C. Martin Perez, M.T. Meinhard, F. Micheli, F. Nessi-Tedaldi, J. Niedziela, F. Pauss, V. Perovic, G. Perrin, S. Pigazzini, M.G. Ratti, M. Reichmann, C. Reissel, T. Reitenspiess, B. Ristic, D. Ruini, D.A. Sanz Becerra, M. Schönenberger, V. Stampf, J. Steggemann⁶⁰, R. Wallny, D.H. Zhu

Universität Zürich, Zurich, Switzerland

C. Amsler⁶², P. Bäertschi, C. Botta, D. Brzhechko, M.F. Canelli, K. Cormier, A. De Wit, R. Del Burgo, J.K. Heikkilä, M. Huwiler, A. Jofrehei, B. Kilminster, S. Leontsinis, A. Macchiolo, P. Meiring, V.M. Mikuni, U. Molinatti, I. Neutelings, A. Reimers, P. Robmann, S. Sanchez Cruz, K. Schweiger, Y. Takahashi

National Central University, Chung-Li, Taiwan

C. Adloff⁶³, C.M. Kuo, W. Lin, A. Roy, T. Sarkar³⁴, S.S. Yu

National Taiwan University (NTU), Taipei, Taiwan

L. Ceard, Y. Chao, K.F. Chen, P.H. Chen, W.-S. Hou, Y.y. Li, R.-S. Lu, E. Paganis, A. Psallidas, A. Steen, H.y. Wu, E. Yazgan, P.r. Yu

Chulalongkorn University, Faculty of Science, Department of Physics, Bangkok, Thailand

B. Asavapibhop, C. Asawatangtrakuldee, N. Srimanobhas

Çukurova University, Physics Department, Science and Art Faculty, Adana, Turkey

F. Boran, S. Damarseckin⁶⁴, Z.S. Demiroglu, F. Dolek, I. Dumanoglu⁶⁵, E. Eskut, Y. Guler, E. Gurpinar Guler⁶⁶, I. Hos⁶⁷, C. Isik, O. Kara, A. Kayis Topaksu, U. Kiminsu, G. Onengut, K. Ozdemir⁶⁸, A. Polatoz, A.E. Simsek, B. Tali⁶⁹, U.G. Tok, S. Turkcapar, I.S. Zorbakir, C. Zorbilmez

Middle East Technical University, Physics Department, Ankara, Turkey

B. Isildak⁷⁰, G. Karapinar⁷¹, K. Ocalan⁷², M. Yalvac⁷³

Bogazici University, Istanbul, Turkey

B. Akgun, I.O. Atakisi, E. Gülmez, M. Kaya⁷⁴, O. Kaya⁷⁵, Ö. Özçelik, S. Tekten⁷⁶, E.A. Yetkin⁷⁷

Istanbul Technical University, Istanbul, Turkey

A. Cakir, K. Cankocak⁶⁵, Y. Komurcu, S. Sen⁷⁸

Istanbul University, Istanbul, Turkey

S. Cerci⁶⁹, B. Kaynak, S. Ozkorucuklu, D. Sunar Cerci⁶⁹

Institute for Scintillation Materials of National Academy of Science of Ukraine, Kharkov, Ukraine

B. Grynyov

National Scientific Center, Kharkov Institute of Physics and Technology, Kharkov, Ukraine

L. Levchuk

University of Bristol, Bristol, United Kingdom

D. Anthony, E. Bhal, S. Bologna, J.J. Brooke, A. Bundock, E. Clement, D. Cussans, H. Flacher,

J. Goldstein, G.P. Heath, H.F. Heath, L. Kreczko, B. Krikler, S. Paramesvaran, S. Seif El Nasr-Storey, V.J. Smith, N. Stylianou⁷⁹, R. White

Rutherford Appleton Laboratory, Didcot, United Kingdom

K.W. Bell, A. Belyaev⁸⁰, C. Brew, R.M. Brown, D.J.A. Cockerill, K.V. Ellis, K. Harder, S. Harper, J. Linacre, K. Manolopoulos, D.M. Newbold, E. Olaiya, D. Petyt, T. Reis, T. Schuh, C.H. Shepherd-Themistocleous, I.R. Tomalin, T. Williams

Imperial College, London, United Kingdom

R. Bainbridge, P. Bloch, S. Bonomally, J. Borg, S. Breeze, O. Buchmuller, V. Cepaitis, G.S. Chahal⁸¹, D. Colling, P. Dauncey, G. Davies, M. Della Negra, S. Fayer, G. Fedi, G. Hall, M.H. Hassanshahi, G. Iles, J. Langford, L. Lyons, A.-M. Magnan, S. Malik, A. Martelli, J. Nash⁸², M. Pesaresi, D.M. Raymond, A. Richards, A. Rose, E. Scott, C. Seez, A. Shtipliyski, A. Tapper, K. Uchida, T. Virdee¹⁷, N. Wardle, S.N. Webb, D. Winterbottom, A.G. Zecchinelli

Brunel University, Uxbridge, United Kingdom

K. Coldham, J.E. Cole, A. Khan, P. Kyberd, I.D. Reid, L. Teodorescu, S. Zahid

Baylor University, Waco, USA

S. Abdullin, A. Brinkerhoff, B. Caraway, J. Dittmann, K. Hatakeyama, A.R. Kanuganti, B. McMaster, N. Pastika, S. Sawant, C. Sutantawibul, J. Wilson

Catholic University of America, Washington, DC, USA

R. Bartek, A. Dominguez, R. Uniyal, A.M. Vargas Hernandez

The University of Alabama, Tuscaloosa, USA

A. Buccilli, S.I. Cooper, D. Di Croce, S.V. Gleyzer, C. Henderson, C.U. Perez, P. Rumerio⁸³, C. West

Boston University, Boston, USA

A. Akpinar, A. Albert, D. Arcaro, C. Cosby, Z. Demiragli, E. Fontanesi, D. Gastler, J. Rohlf, K. Salyer, D. Sperka, D. Spitzbart, I. Suarez, A. Tsatsos, S. Yuan, D. Zou

Brown University, Providence, USA

G. Benelli, B. Burkle, X. Coubez¹⁸, D. Cutts, M. Hadley, U. Heintz, J.M. Hogan⁸⁴, G. Landsberg, K.T. Lau, M. Lukasik, J. Luo, M. Narain, S. Sagir⁸⁵, E. Usai, W.Y. Wong, X. Yan, D. Yu, W. Zhang

University of California, Davis, Davis, USA

J. Bonilla, C. Brainerd, R. Breedon, M. Calderon De La Barca Sanchez, M. Chertok, J. Conway, P.T. Cox, R. Erbacher, G. Haza, F. Jensen, O. Kukral, R. Lander, M. Mulhearn, D. Pellett, B. Regnery, D. Taylor, Y. Yao, F. Zhang

University of California, Los Angeles, USA

M. Bachtis, R. Cousins, A. Datta, D. Hamilton, J. Hauser, M. Ignatenko, M.A. Iqbal, T. Lam, N. Mccoll, W.A. Nash, S. Regnard, D. Saltzberg, B. Stone, V. Valuev

University of California, Riverside, Riverside, USA

K. Burt, Y. Chen, R. Clare, J.W. Gary, M. Gordon, G. Hanson, G. Karapostoli, O.R. Long, N. Manganeli, M. Olmedo Negrete, W. Si, S. Wimpenny, Y. Zhang

University of California, San Diego, La Jolla, USA

J.G. Branson, P. Chang, S. Cittolin, S. Cooperstein, N. Deelen, J. Duarte, R. Gerosa, L. Giannini, D. Gilbert, J. Guiang, R. Kansal, V. Krutelyov, R. Lee, J. Letts, M. Masciovecchio, S. May, M. Pieri, B.V. Sathia Narayanan, V. Sharma, M. Tadel, A. Vartak, F. Würthwein, Y. Xiang, A. Yagil

University of California, Santa Barbara - Department of Physics, Santa Barbara, USA

N. Amin, C. Campagnari, M. Citron, A. Dorsett, V. Dutta, J. Incandela, M. Kilpatrick, J. Kim, B. Marsh, H. Mei, M. Oshiro, M. Quinnan, J. Richman, U. Sarica, D. Stuart, S. Wang

California Institute of Technology, Pasadena, USA

A. Bornheim, O. Cerri, I. Dutta, J.M. Lawhorn, N. Lu, J. Mao, H.B. Newman, J. Ngadiuba, T.Q. Nguyen, M. Spiropulu, J.R. Vlimant, C. Wang, S. Xie, Z. Zhang, R.Y. Zhu

Carnegie Mellon University, Pittsburgh, USA

J. Alison, S. An, M.B. Andrews, P. Bryant, T. Ferguson, A. Harilal, C. Liu, T. Mudholkar, M. Paulini, A. Sanchez

University of Colorado Boulder, Boulder, USA

J.P. Cumalat, W.T. Ford, A. Hassani, E. MacDonald, R. Patel, A. Perloff, C. Savard, K. Stenson, K.A. Ulmer, S.R. Wagner

Cornell University, Ithaca, USA

J. Alexander, Y. Cheng, D.J. Cranshaw, S. Hogan, J. Monroy, J.R. Patterson, D. Quach, J. Reichert, A. Ryd, W. Sun, J. Thom, P. Wittich, R. Zou

Fermi National Accelerator Laboratory, Batavia, USA

M. Albrow, M. Alyari, G. Apollinari, A. Apresyan, A. Apyan, S. Banerjee, L.A.T. Bauerdick, D. Berry, J. Berryhill, P.C. Bhat, K. Burkett, J.N. Butler, A. Canepa, G.B. Cerati, H.W.K. Cheung, F. Chlebana, M. Cremonesi, K.F. Di Petrillo, V.D. Elvira, Y. Feng, J. Freeman, Z. Gecse, L. Gray, D. Green, S. Grünendahl, O. Gutsche, R.M. Harris, R. Heller, T.C. Herwig, J. Hirschauer, B. Jayatilaka, S. Jindariani, M. Johnson, U. Joshi, T. Klijnsma, B. Klima, K.H.M. Kwok, S. Lammel, D. Lincoln, R. Lipton, T. Liu, C. Madrid, K. Maeshima, C. Mantilla, D. Mason, P. McBride, P. Merkel, S. Mrenna, S. Nahn, V. O'Dell, V. Papadimitriou, K. Pedro, C. Pena⁵⁴, O. Prokofyev, F. Ravera, A. Reinsvold Hall, L. Ristori, B. Schneider, E. Sexton-Kennedy, N. Smith, A. Soha, W.J. Spalding, L. Spiegel, S. Stoynev, J. Strait, L. Taylor, S. Tkaczyk, N.V. Tran, L. Uplegger, E.W. Vaandering, H.A. Weber

University of Florida, Gainesville, USA

D. Acosta, P. Avery, D. Bourilkov, L. Cadamuro, V. Cherepanov, F. Errico, R.D. Field, D. Guerrero, B.M. Joshi, M. Kim, E. Koenig, J. Konigsberg, A. Korytov, K.H. Lo, K. Matchev, N. Menendez, G. Mitselmakher, A. Muthirakalayil Madhu, N. Rawal, D. Rosenzweig, S. Rosenzweig, K. Shi, J. Sturdy, J. Wang, E. Yigitbasi, X. Zuo

Florida State University, Tallahassee, USA

T. Adams, A. Askew, D. Diaz, R. Habibullah, V. Hagopian, K.F. Johnson, R. Khurana, T. Kolberg, G. Martinez, H. Prosper, C. Schiber, R. Yohay, J. Zhang

Florida Institute of Technology, Melbourne, USA

M.M. Baarmand, S. Butalla, T. Elkafrawy⁸⁶, M. Hohlmann, R. Kumar Verma, D. Noonan, M. Rahmani, M. Saunders, F. Yumiceva

University of Illinois at Chicago (UIC), Chicago, USA

M.R. Adams, H. Becerril Gonzalez, R. Cavanaugh, X. Chen, S. Dittmer, O. Evdokimov, C.E. Gerber, D.A. Hangal, D.J. Hofman, A.H. Merrit, C. Mills, G. Oh, T. Roy, S. Rudrabhatla, M.B. Tonjes, N. Varelas, J. Viinikainen, X. Wang, Z. Wu, Z. Ye

The University of Iowa, Iowa City, USA

M. Alhousseini, K. Dilsiz⁸⁷, R.P. Gandrajula, O.K. Köseyan, J.-P. Merlo, A. Mestvirishvili⁸⁸, J. Nachtman, H. Ogul⁸⁹, Y. Onel, A. Penzo, C. Snyder, E. Tiras⁹⁰

Johns Hopkins University, Baltimore, USA

O. Amram, B. Blumenfeld, L. Corcodilos, J. Davis, M. Eminizer, A.V. Gritsan, S. Kyriacou, P. Maksimovic, J. Roskes, M. Swartz, T.Á. Vámi

The University of Kansas, Lawrence, USA

J. Anguiano, C. Baldenegro Barrera, P. Baringer, A. Bean, A. Bylinkin, T. Isidori, S. Khalil, J. King, G. Krintiras, A. Kropivnitskaya, C. Lindsey, N. Minafra, M. Murray, C. Rogan, C. Royon, S. Sanders, E. Schmitz, C. Smith, J.D. Tapia Takaki, Q. Wang, J. Williams, G. Wilson

Kansas State University, Manhattan, USA

S. Duric, A. Ivanov, K. Kaadze, D. Kim, Y. Maravin, T. Mitchell, A. Modak, K. Nam

Lawrence Livermore National Laboratory, Livermore, USA

F. Rebasoo, D. Wright

University of Maryland, College Park, USA

E. Adams, A. Baden, O. Baron, A. Belloni, S.C. Eno, N.J. Hadley, S. Jabeen, R.G. Kellogg, T. Koeth, A.C. Mignerey, S. Nabili, M. Seidel, A. Skuja, L. Wang, K. Wong

Massachusetts Institute of Technology, Cambridge, USA

D. Abercrombie, G. Andreassi, R. Bi, S. Brandt, W. Busza, I.A. Cali, Y. Chen, M. D'Alfonso, J. Eysermans, G. Gomez Ceballos, M. Goncharov, P. Harris, M. Hu, M. Klute, D. Kovalskyi, J. Krupa, Y.-J. Lee, B. Maier, C. Mironov, C. Paus, D. Rankin, C. Roland, G. Roland, Z. Shi, G.S.F. Stephans, K. Tatar, J. Wang, Z. Wang, B. Wyslouch

University of Minnesota, Minneapolis, USA

R.M. Chatterjee, A. Evans, P. Hansen, J. Hiltbrand, Sh. Jain, M. Krohn, Y. Kubota, J. Mans, M. Revering, R. Rusack, R. Saradhy, N. Schroeder, N. Strobbe, M.A. Wadud

University of Nebraska-Lincoln, Lincoln, USA

K. Bloom, M. Bryson, S. Chauhan, D.R. Claes, C. Fangmeier, L. Finco, F. Golf, J.R. González Fernández, C. Joo, I. Kravchenko, M. Musich, I. Reed, J.E. Siado, G.R. Snow[†], W. Tabb, F. Yan

State University of New York at Buffalo, Buffalo, USA

G. Agarwal, H. Bandyopadhyay, L. Hay, I. Iashvili, A. Kharchilava, C. McLean, D. Nguyen, J. Pekkanen, S. Rappoccio, A. Williams

Northeastern University, Boston, USA

G. Alverson, E. Barberis, C. Freer, Y. Haddad, A. Hortiangtham, J. Li, G. Madigan, B. Marzocchi, D.M. Morse, V. Nguyen, T. Orimoto, A. Parker, L. Skinnari, A. Tishelman-Charny, T. Wamorkar, B. Wang, A. Wisecarver, D. Wood

Northwestern University, Evanston, USA

S. Bhattacharya, J. Bueghly, Z. Chen, A. Gilbert, T. Gunter, K.A. Hahn, N. Odell, M.H. Schmitt, M. Velasco

University of Notre Dame, Notre Dame, USA

R. Band, R. Bucci, A. Das, N. Dev, R. Goldouzian, M. Hildreth, K.W. Ho, K. Hurtado Anampa, C. Jessop, K. Lannon, N. Loukas, N. Marinelli, I. Mcalister, T. McCauley, F. Meng, K. Mohrman, Y. Musienko⁴⁶, R. Ruchti, P. Siddireddy, S. Taroni, M. Wayne, A. Wightman, M. Wolf, M. Zarucki, L. Zygala

The Ohio State University, Columbus, USA

B. Bylsma, B. Cardwell, L.S. Durkin, B. Francis, C. Hill, M. Nunez Ornelas, K. Wei, B.L. Winer, B.R. Yates

Princeton University, Princeton, USA

F.M. Addesa, B. Bonham, P. Das, G. Dezoort, P. Elmer, A. Frankenthal, B. Greenberg, N. Haubrich, S. Higginbotham, A. Kalogeropoulos, G. Kopp, S. Kwan, D. Lange, M.T. Lucchini, D. Marlow, K. Mei, I. Ojalvo, J. Olsen, C. Palmer, D. Stickland, C. Tully

University of Puerto Rico, Mayaguez, USA

S. Malik, S. Norberg

Purdue University, West Lafayette, USA

A.S. Bakshi, V.E. Barnes, R. Chawla, S. Das, L. Gutay, M. Jones, A.W. Jung, S. Karmarkar, M. Liu, G. Negro, N. Neumeister, G. Paspalaki, C.C. Peng, S. Piperov, A. Purohit, J.F. Schulte, M. Stojanovic¹⁴, J. Thieman, F. Wang, R. Xiao, W. Xie

Purdue University Northwest, Hammond, USA

J. Dolen, N. Parashar

Rice University, Houston, USA

A. Baty, M. Decaro, S. Dildick, K.M. Ecklund, S. Freed, P. Gardner, F.J.M. Geurts, A. Kumar, W. Li, B.P. Padley, R. Redjimi, W. Shi, A.G. Stahl Leitton, S. Yang, L. Zhang, Y. Zhang

University of Rochester, Rochester, USA

A. Bodek, P. de Barbaro, R. Demina, J.L. Dulemba, C. Fallon, T. Ferbel, M. Galanti, A. Garcia-Bellido, O. Hindrichs, A. Khukhunaishvili, E. Ranken, R. Taus

Rutgers, The State University of New Jersey, Piscataway, USA

B. Chiarito, J.P. Chou, A. Gandrakota, Y. Gershtein, E. Halkiadakis, A. Hart, M. Heindl, E. Hughes, S. Kaplan, O. Karacheban²¹, I. Laflotte, A. Lath, R. Montalvo, K. Nash, M. Osherson, S. Salur, S. Schnetzer, S. Somalwar, R. Stone, S.A. Thayil, S. Thomas, H. Wang

University of Tennessee, Knoxville, USA

H. Acharya, A.G. Delannoy, S. Spanier

Texas A&M University, College Station, USA

O. Bouhali⁹¹, M. Dalchenko, A. Delgado, R. Eusebi, J. Gilmore, T. Huang, T. Kamon⁹², H. Kim, S. Luo, S. Malhotra, R. Mueller, D. Overton, D. Rathjens, A. Safonov

Texas Tech University, Lubbock, USA

N. Akchurin, J. Damgov, V. Hegde, S. Kunori, K. Lamichhane, S.W. Lee, T. Mengke, S. Muthumuni, T. Peltola, I. Volobouev, Z. Wang, A. Whitbeck

Vanderbilt University, Nashville, USA

E. Appelt, S. Greene, A. Gurrola, W. Johns, A. Melo, H. Ni, K. Padeken, F. Romeo, P. Sheldon, S. Tuo, J. Velkovska

University of Virginia, Charlottesville, USA

M.W. Arenton, B. Cox, G. Cummings, J. Hakala, R. Hirosky, M. Joyce, A. Ledovskoy, A. Li, C. Neu, B. Tannenwald, S. White, E. Wolfe

Wayne State University, Detroit, USA

N. Poudyal

University of Wisconsin - Madison, Madison, WI, USA

K. Black, T. Bose, J. Buchanan, C. Caillol, S. Dasu, I. De Bruyn, P. Everaerts, F. Fienga, C. Galloni, H. He, M. Herndon, A. Hervé, U. Hussain, A. Lanaro, A. Loeliger, R. Loveless, J. Madhusudanan Sreekala, A. Mallampalli, A. Mohammadi, D. Pinna, A. Savin, V. Shang, V. Sharma, W.H. Smith, D. Teague, S. Trembath-reichert, W. Vetens

†: Deceased

1: Also at TU Wien, Wien, Austria

2: Also at Institute of Basic and Applied Sciences, Faculty of Engineering, Arab Academy for Science, Technology and Maritime Transport, Alexandria, Egypt, Alexandria, Egypt

3: Also at Université Libre de Bruxelles, Bruxelles, Belgium

4: Also at Universidade Estadual de Campinas, Campinas, Brazil

5: Also at Federal University of Rio Grande do Sul, Porto Alegre, Brazil

6: Also at University of Chinese Academy of Sciences, Beijing, China

7: Also at Department of Physics, Tsinghua University, Beijing, China, Beijing, China

8: Also at UFMS, Nova Andradina, Brazil

9: Also at Nanjing Normal University Department of Physics, Nanjing, China

10: Now at The University of Iowa, Iowa City, USA

11: Also at Institute for Theoretical and Experimental Physics named by A.I. Alikhanov of NRC 'Kurchatov Institute', Moscow, Russia

12: Also at Joint Institute for Nuclear Research, Dubna, Russia

13: Also at Cairo University, Cairo, Egypt

14: Also at Purdue University, West Lafayette, USA

15: Also at Université de Haute Alsace, Mulhouse, France

16: Also at Erzincan Binali Yildirim University, Erzincan, Turkey

17: Also at CERN, European Organization for Nuclear Research, Geneva, Switzerland

18: Also at RWTH Aachen University, III. Physikalisches Institut A, Aachen, Germany

19: Also at University of Hamburg, Hamburg, Germany

20: Also at Department of Physics, Isfahan University of Technology, Isfahan, Iran, Isfahan, Iran

21: Also at Brandenburg University of Technology, Cottbus, Germany

22: Also at Skobeltsyn Institute of Nuclear Physics, Lomonosov Moscow State University, Moscow, Russia

23: Also at Physics Department, Faculty of Science, Assiut University, Assiut, Egypt

24: Also at Eszterhazy Karoly University, Karoly Robert Campus, Gyongyos, Hungary

25: Also at Institute of Physics, University of Debrecen, Debrecen, Hungary, Debrecen, Hungary

26: Also at Institute of Nuclear Research ATOMKI, Debrecen, Hungary

27: Also at MTA-ELTE Lendület CMS Particle and Nuclear Physics Group, Eötvös Loránd University, Budapest, Hungary, Budapest, Hungary

28: Also at Wigner Research Centre for Physics, Budapest, Hungary

29: Also at IIT Bhubaneswar, Bhubaneswar, India, Bhubaneswar, India

30: Also at Institute of Physics, Bhubaneswar, India

31: Also at G.H.G. Khalsa College, Punjab, India

32: Also at Shoolini University, Solan, India

33: Also at University of Hyderabad, Hyderabad, India

34: Also at University of Visva-Bharati, Santiniketan, India

35: Also at Indian Institute of Technology (IIT), Mumbai, India

36: Also at Deutsches Elektronen-Synchrotron, Hamburg, Germany

37: Also at Sharif University of Technology, Tehran, Iran

-
- 38: Also at Department of Physics, University of Science and Technology of Mazandaran, Behshahr, Iran
- 39: Now at INFN Sezione di Bari ^a, Università di Bari ^b, Politecnico di Bari ^c, Bari, Italy
- 40: Also at Italian National Agency for New Technologies, Energy and Sustainable Economic Development, Bologna, Italy
- 41: Also at Centro Siciliano di Fisica Nucleare e di Struttura Della Materia, Catania, Italy
- 42: Also at Università di Napoli 'Federico II', NAPOLI, Italy
- 43: Also at Riga Technical University, Riga, Latvia, Riga, Latvia
- 44: Also at Consejo Nacional de Ciencia y Tecnología, Mexico City, Mexico
- 45: Also at IRFU, CEA, Université Paris-Saclay, Gif-sur-Yvette, France
- 46: Also at Institute for Nuclear Research, Moscow, Russia
- 47: Now at National Research Nuclear University 'Moscow Engineering Physics Institute' (MEPhI), Moscow, Russia
- 48: Also at Institute of Nuclear Physics of the Uzbekistan Academy of Sciences, Tashkent, Uzbekistan
- 49: Also at St. Petersburg State Polytechnical University, St. Petersburg, Russia
- 50: Also at University of Florida, Gainesville, USA
- 51: Also at Imperial College, London, United Kingdom
- 52: Also at P.N. Lebedev Physical Institute, Moscow, Russia
- 53: Also at Moscow Institute of Physics and Technology, Moscow, Russia, Moscow, Russia
- 54: Also at California Institute of Technology, Pasadena, USA
- 55: Also at Budker Institute of Nuclear Physics, Novosibirsk, Russia
- 56: Also at Faculty of Physics, University of Belgrade, Belgrade, Serbia
- 57: Also at Trincomalee Campus, Eastern University, Sri Lanka, Nilaveli, Sri Lanka
- 58: Also at INFN Sezione di Pavia ^a, Università di Pavia ^b, Pavia, Italy, Pavia, Italy
- 59: Also at National and Kapodistrian University of Athens, Athens, Greece
- 60: Also at Ecole Polytechnique Fédérale Lausanne, Lausanne, Switzerland
- 61: Also at Universität Zürich, Zurich, Switzerland
- 62: Also at Stefan Meyer Institute for Subatomic Physics, Vienna, Austria, Vienna, Austria
- 63: Also at Laboratoire d'Annecy-le-Vieux de Physique des Particules, IN2P3-CNRS, Annecy-le-Vieux, France
- 64: Also at Şırnak University, Sirnak, Turkey
- 65: Also at Near East University, Research Center of Experimental Health Science, Nicosia, Turkey
- 66: Also at Konya Technical University, Konya, Turkey
- 67: Also at Istanbul University - Cerrahpasa, Faculty of Engineering, Istanbul, Turkey
- 68: Also at Piri Reis University, Istanbul, Turkey
- 69: Also at Adiyaman University, Adiyaman, Turkey
- 70: Also at Ozyegin University, Istanbul, Turkey
- 71: Also at Izmir Institute of Technology, Izmir, Turkey
- 72: Also at Necmettin Erbakan University, Konya, Turkey
- 73: Also at Bozok Universitetesi Rektörlüğü, Yozgat, Turkey, Yozgat, Turkey
- 74: Also at Marmara University, Istanbul, Turkey
- 75: Also at Milli Savunma University, Istanbul, Turkey
- 76: Also at Kafkas University, Kars, Turkey
- 77: Also at Istanbul Bilgi University, Istanbul, Turkey
- 78: Also at Hacettepe University, Ankara, Turkey
- 79: Also at Vrije Universiteit Brussel, Brussel, Belgium
- 80: Also at School of Physics and Astronomy, University of Southampton, Southampton,

United Kingdom

- 81: Also at IPPP Durham University, Durham, United Kingdom
- 82: Also at Monash University, Faculty of Science, Clayton, Australia
- 83: Also at Università di Torino, TORINO, Italy
- 84: Also at Bethel University, St. Paul, Minneapolis, USA, St. Paul, USA
- 85: Also at Karamanoğlu Mehmetbey University, Karaman, Turkey
- 86: Also at Ain Shams University, Cairo, Egypt
- 87: Also at Bingol University, Bingol, Turkey
- 88: Also at Georgian Technical University, Tbilisi, Georgia
- 89: Also at Sinop University, Sinop, Turkey
- 90: Also at Erciyes University, KAYSERI, Turkey
- 91: Also at Texas A&M University at Qatar, Doha, Qatar
- 92: Also at Kyungpook National University, Daegu, Korea, Daegu, Korea